



The Parvalbumin Hypothesis of Autism Spectrum Disorder

*Federica Filice, Lucia Janickova, Thomas Henzi, Alessandro Bilella and Beat Schwaller**

Section of Medicine, Anatomy, University of Fribourg, Fribourg, Switzerland

OPEN ACCESS

Edited by:

Yu-Chih Lin,
Husman Institute for Autism,
United States

Reviewed by:

Nael Nadif Kasri,
Radboud University
Nijmegen, Netherlands
Christopher Pittenger,
Yale University, United States
Rochelle Marie Hines,
University of Nevada, Las Vegas,
United States

*Correspondence:

Beat Schwaller
beat.schwaller@unifr.ch

Specialty section:

This article was submitted to
Cellular Neuropathology,
a section of the journal
Frontiers in Cellular Neuroscience

Received: 29 June 2020

Accepted: 10 November 2020

Published: 18 December 2020

Citation:

Filice F, Janickova L, Henzi T, Bilella A
and Schwaller B (2020) The
Parvalbumin Hypothesis of Autism
Spectrum Disorder.
Front. Cell. Neurosci. 14:577525.
doi: 10.3389/fncel.2020.577525

The prevalence of autism spectrum disorder (ASD)—a type of neurodevelopmental disorder—is increasing and is around 2% in North America, Asia, and Europe. Besides the known genetic link, environmental, epigenetic, and metabolic factors have been implicated in ASD etiology. Although highly heterogeneous at the behavioral level, ASD comprises a set of core symptoms including impaired communication and social interaction skills as well as stereotyped and repetitive behaviors. This has led to the suggestion that a large part of the ASD phenotype is caused by changes in a few and common set of signaling pathways, the identification of which is a fundamental aim of autism research. Using advanced bioinformatics tools and the abundantly available genetic data, it is possible to classify the large number of ASD-associated genes according to cellular function and pathways. Cellular processes known to be impaired in ASD include gene regulation, synaptic transmission affecting the excitation/inhibition balance, neuronal Ca²⁺ signaling, development of short-/long-range connectivity (circuits and networks), and mitochondrial function. Such alterations often occur during early postnatal neurodevelopment. Among the neurons most affected in ASD as well as in schizophrenia are those expressing the Ca²⁺-binding protein parvalbumin (PV). These mainly inhibitory interneurons present in many different brain regions in humans and rodents are characterized by rapid, non-adaptive firing and have a high energy requirement. PV expression is often reduced at both messenger RNA (mRNA) and protein levels in human ASD brain samples and mouse ASD (and schizophrenia) models. Although the human *PVALB* gene is not a high-ranking susceptibility/risk gene for either disorder and is currently only listed in the SFARI Gene Archive, we propose and present supporting evidence for the Parvalbumin Hypothesis, which posits that decreased PV level is causally related to the etiology of ASD (and possibly schizophrenia).

Keywords: parvalbumin, autism (ASD), calcium signal modulator, GABAergic neurons, E/I balance, schizophrenia, ROS, mitochondria

INTRODUCTION

Complex mechanisms underlie neurodevelopmental disorders (NDDs) and neuropsychiatric conditions. From the molecular to the system level, subtle changes at any point during development can lead to impairment of brain functions including cognition, learning, memory, and behavior, which are dynamic and subject to developmental and environmental influences and activity/experience-dependent mechanisms. Genome-wide association studies, investigation of rare genetic disorders, and transcriptome analyses aim to identify genes implicated in the etiology of NDDs, and bioinformatics approaches are used to elucidate dysregulated processes/pathways.

The interplay between altered genes, circuits, and networks giving rise to clinical symptoms in NDDs is illustrated in Figure 1 of Krol et al. (2018).

The motivation for the present article comes from many studies on ASD and schizophrenia focusing on the calcium-binding protein parvalbumin (PV) expressed by a subpopulation of neurons (sometimes referred to as fast-spiking interneurons (FSIs) or PV⁺ interneurons; Hu et al., 2014). There is some confusion in the literature regarding the nomenclature. In most morphological studies using immunohistochemical methods, PV⁺ neurons are defined as those labeled by anti-PV antibody. A case where the number of PV-immunoreactive neurons is lower than in control animals as a result of experimental treatment or genetic manipulation is either correctly described as a reduction in the number of PV⁺ neurons or otherwise as a loss of PV⁺ neurons. The latter implies that these neurons either died or did not properly migrate to a specific brain region during development as a result of the manipulation, while a third possibility is that PV was downregulated to a level below the limit of detection by immunohistochemistry (IHC). Thus, distinguishing between PV⁺ neuron loss vs. decreased PV expression is critical for accurately interpreting previous studies. For the remainder of this article, we use the term PV⁺ neurons only in reference to neurons identified solely by PV IHC; the class of interneurons defined by PV expression as well as additional features (e.g., morphology, electrophysiological properties, and transcriptome profile) is referred to as Pvalb neurons irrespective of PV expression level. As an example, brains of PV^{-/-} mice completely lacking PV expression were found to harbor the same number of Pvalb neurons as wild-type (WT) mice (Filice et al., 2016).

The Parvalbumin Hypothesis of ASD was formulated based on the following lines of evidence: (1) the function of Pvalb neurons is often impaired in NDDs and neuropsychiatric disorders (Marin, 2012; Ferguson and Gao, 2018; Selten et al., 2018); (2) *PVALB* mRNA is the most strongly downregulated transcript in human ASD samples (Schwede et al., 2018); (3) the number of PV⁺ neurons is decreased in sections of human ASD brain (Hashemi et al., 2017; Ariza et al., 2018); and (4) transgenic mice with lower (PV^{+/-}) or absent (PV^{-/-}) expression exhibit the core ASD-like symptoms (Wöhr et al., 2015); the main points of the Parvalbumin Hypothesis are graphically summarized in Figure 1.

DATA SUPPORTING THE PARVALBUMIN HYPOTHESIS OF ASD

Decreased Number of PV⁺ Neurons in Human ASD Postmortem Brains: Pvalb Neuron Loss vs. PV Downregulation

The cerebral cortex harbors several classes of interneurons including Pvalb neurons. Early classification of these neurons was based on their morphology [most notably of the axon (Kawaguchi and Kubota, 1997; Toledo-Rodriguez et al., 2005)], firing pattern, PV expression, and gene expression profile determined by PCR (Toledo-Rodriguez et al., 2004). More

recent classifications based on single-cell or single-nucleus RNA-sequencing (RNA-seq) (Hodge et al., 2019), patch sequencing (Patch-seq) yielding morphoelectric (*met*-type) and transcriptomic (*t*-type) datasets (Gouwens et al., 2020), or machine learning applied to a large patch-seq dataset (Gala et al., 2020) have identified 7 clusters (RNA-seq) as well as 10 *t*-type and 5 *met*-type (patch-seq) Pvalb neurons. Given the different algorithms used to stratify the datasets, it is not surprising that the reported number of Pvalb neuron subtypes varies across studies. Pvalb neurons in the cortex include several types of basket cell, chandelier cell, and translaminal neurons. Basket cells localized in layers 2–6 constitute the majority; chandelier cells are abundant at the boundary between layers 1 and 2 and in layer 6; and the relatively rare translaminal Pvalb neurons are mostly present in layers 5 and 6 (Lim et al., 2018). A similar classification has been applied to hippocampal Pvalb neurons (Somogyi and Klausberger, 2005).

In order to conclude that PV⁺ neurons are absent in postmortem ASD brains, it must be demonstrated that neurons with specific morphoelectric, transcriptomic, and biochemical properties are missing/reduced. The typically fixed postmortem human brain tissue samples preclude the assessment of these properties. Besides non-adaptive firing, PV⁺ neurons are characterized by PV expression. However, the complete absence of PV cannot be taken as evidence that Pvalb neurons are absent, which must be determined based on the expression of other Pvalb neuron-specific markers including voltage-gated potassium channel Kv3.1b (*KCNK1*), potassium voltage-gated channel modifier subfamily S member 3 Kv9.3 (*KCNK3*), or components of perineuronal nets (PNNs), which are a set of extracellular matrix molecules surrounding Pvalb neurons in several brain regions including the cortex (Celio et al., 1998). The presence and/or intensity of PNN immunolabeling must be interpreted with caution because PNN components, like other Pvalb neuron markers besides PV (*PVALB*)—e.g., *GAD67* (*GAD1*)—are regulated in an experience/activity-dependent manner (Cohen et al., 2016), and their expression changes over the course of development (Wang and Fawcett, 2012; Ye and Miao, 2013). Earlier studies found no significant changes in the number of PV⁺ or calbindin-D28K-positive (CB⁺) neurons in the posterior cingulate cortex and fusiform gyrus of postmortem ASD brains (Oblak et al., 2011). However, the mean density of PV⁺ neurons was slightly reduced in the superficial and deep layers of both of these areas. In another study, the density of PV⁺ cerebellar stellate and basket cells did not differ significantly between ASD ($n = 6$) and control ($n = 4$) samples, although the number of Purkinje cells was reduced in two or three ASD samples (Whitney et al., 2009). Moreover, the mean neuron density of both interneuron subtypes was reduced (basket cells, -15%; stellate cells, -5%), although the difference was not statistically significant. These findings imply that the number of PV⁺ neurons is decreased or PV is downregulated in ASD. In a preliminary study (Zikopoulos and Barbas, 2013) comparing the density of CB⁺ and PV⁺ cortical interneurons in postmortem adult human brain tissue (ASD and control; $n = 2$) from dorsolateral prefrontal area 9, a significant reduction in the number of PV⁺ neurons was observed in ASD brains; the ratio of

equally found in the supra- and infragranular layers. The authors speculated that the decrease in PV⁺ neurons was due to the loss of Pvalb neurons or downregulation of PV protein expression. In a follow-up study (Ariza et al., 2018), PV⁺ interneuron subtypes (basket and chandelier cells) were separately analyzed in the same samples (Hashemi et al., 2018); double immunolabeling of PV and PNNs with *Vicia villosa agglutinin* (VVA) enabled the differentiation of basket and chandelier cells, as only the former are surrounded by VVA⁺ PNNs in human brain. The number of PV⁺ chandelier cells was consistently lower in the PFC of ASD specimens ($n = 10$); the number of PV⁺/VVA⁺ basket cells was also reduced but to a lesser degree. As the authors did not use a second marker to unambiguously identify chandelier cells, they concluded that the reduction in the number of PV⁺ cells represents either a true loss of Pvalb neurons (mostly chandelier cells) or a decrease in PV protein level.

PV expression is developmentally regulated in humans and rodents. It has been suggested that gene expression changes in NDDs are related to an immature developmental gene expression program of PV⁺ FSIs (Gandal et al., 2012). Cell-type-specific maturation indices calculated from microarray datasets showed that the index for Pvalb neurons was highly correlated with PV expression level in these cells. In all three analyzed diseases (ASD, schizophrenia, and bipolar disorder), the maturation index and PV expression level were significantly reduced, consistent with a delayed/impaired developmental gene expression program. While there are currently no quantitative data on PV expression in human ASD brains, *PVALB* mRNA level has been measured in several studies. Radioisotopic *in situ* hybridization in postmortem brains of ASD and control cases revealed that *PVALB* transcript level was downregulated in cerebellar Purkinje cells of ASD brains, independent of postmortem interval or age at death (Soghomonian et al., 2017). An examination of neocortical architecture in postmortem brain specimens of autistic and normal children aged between 2 and 15 years revealed discrete patches of abnormal and disorganized laminar cytoarchitecture in most samples (Stoner et al., 2014). An analysis of specific molecular markers by RNA *in situ* hybridization showed abnormal gene expression in these neocortical regions: the level of the interneuron marker *PVALB* was decreased, whereas no difference was observed in the total number of neurons by Nissl staining. In accordance with the *in situ* hybridization data, analyses of an RNA-seq dataset (Parikshak et al., 2016) and three microarray datasets (Garbett et al., 2008; Voineagu et al., 2011; Chow et al., 2012) identified *PVALB* mRNA as the most strongly downregulated transcript in the cerebral cortex of ASD patients (Schwede et al., 2018).

The Ca²⁺/CaM-dependent protein kinase (CaMK) pathway is implicated in Ca²⁺/activity-dependent gene expression (Ebert and Greenberg, 2013), including in Pvalb neurons (Cohen et al., 2016). Many neurons are regulated by CaMK II and/or IV (reviewed in Bayer and Schulman, 2019). However, Pvalb neurons use the less common isoform γ CAMK I (*Camk1g*) to induce cAMP response element-binding protein (CREB) phosphorylation and expression of prototypical activity-driven genes (*c-Fos*, *Arc*, and *Wnt2*) as well as *Gad1* and *Pvalb* (Cohen et al., 2016). The observation that the *CAMK1G* transcript is

among the top 40 (out of >250) significantly downregulated mRNAs detected in combined gene array datasets of human ASD samples (Schwede et al., 2018) suggests that impaired activity of Pvalb neurons in ASD results in (likely γ CAMK I-dependent) reduced PV expression. Additionally, coordinated dysregulation of genes implicated in synaptic and mitochondrial functions was observed in ASD specimens (Schwede et al., 2018). The possible link between *PVALB* dysregulation and mitochondria is discussed in greater detail in *Effect of PV on Mitochondria, Oxidative Stress, and Pvalb Neuron Morphology: Link to NDDs*.

In summary, *PVALB* transcript level is not only reduced in the brain of ASD cases compared to normal controls but also shows the strongest downregulation among differentially expressed genes. Regarding Pvalb neuron loss, no study to date has provided definitive evidence (using Pvalb neuron markers such as Kv3.1b or Kv9.3) of a lower number/density of Pvalb neurons in human ASD brains. Even if this was demonstrated, an outstanding question would be whether this is due to the death of true Pvalb neurons (i.e., Pvalb neuron-selective neurodegeneration), defects in migration or maturation of immature Pvalb neurons during development (e.g., as seen in *Dlx5/6*^{-/-} mice; Wang et al., 2010), or another mechanism. The downregulation of PV may be linked to loss of Pvalb neuron function, although a partial decrease in function resulting from the abovementioned processes cannot be excluded.

Animal NDD Models of ASD With Reduced PV Expression and/or Decreased Number/Altered Distribution of PV⁺ Neurons

Various animal models have been used to investigate NDDs including ASD. ASD risk genes are defined as those that are more frequently mutated in ASD patients than is expected by chance. Large-scale exome sequencing has identified 102 such genes (Satterstrom et al., 2020). An animal (mouse) model harboring the same (or similar) mutations and shows ASD-like behavior has high construct validity. However, in recent years, numerous mouse models (inbred, experimentally induced, and transgenic) have been discovered or established that show varying degrees of typical ASD-like core symptoms. A list of such models (>1,000) is available in the SFARI Gene database (<https://gene.sfari.org/>), with genes putatively associated with ASD ranked according to several criteria. More models (>3,000) are listed in the AutDB database (<http://autism.mindspec.org/autdb/Welcome.do>). The number of (mostly mouse) ASD models is constantly increasing, with the models themselves becoming more sophisticated as a result of the possibility of inactivating/deleting genes in a brain region- and neuron type-specific and temporally regulated manner. The last aspect is particularly important for elucidating the etiology of NDDs. Although many mouse models currently used in basic research lack robust construct validity, their strong face validity [anatomic, biochemical, neuropathological, or behavioral phenotype(s) similar to humans] make them highly useful for mechanistic studies on ASD etiology. In this paper, we focus on NDD models affecting Pvalb neurons in terms of neuron number and function and PV expression level,

irrespective whether they are currently classified as models of validated (syndromic) ASD risk genes.

The functional impairment of Pvalb neurons has attracted considerable attention in ASD research (Gogolla et al., 2009; Marin, 2012). The distribution of Pvalb neurons in the rat nervous system has been described before (Celio, 1990). A more detailed and quantitative analysis of Pvalb neuron distribution was carried out using mice in which green fluorescent protein (GFP) fused to histone 2B was selectively expressed in Pvalb neurons (PV-Cre:H2B-GFP) (Kim et al., 2017). In the same study, the distribution of other interneuron classes [somatostatin-positive (SST⁺) and vasoactive intestinal polypeptide-positive (VIP⁺) interneurons] was analyzed in parallel; the results showed an uneven distribution of the three major interneuron types in the isocortex. The density of the different interneuron subtypes varies in different cortical layers (Kim et al., 2017). Known changes in PV expression (mainly determined by IHC) or in Pvalb neuron function (detected by electrophysiological recordings) are summarized in **Table 1**. In many mouse models, PV IHC has revealed an overall reduction in PV⁺ cell numbers in brain regions associated with ASD including the somatosensory cortex (SSC), medial (m)PFC, striatum, hippocampus, thalamic reticular nucleus (TRN), and cerebellum. Importantly, the choice of brain region for investigating PV expression has been somewhat arbitrary and likely dictated by other types of experiments (usually electrophysiology). Thus, if a significant difference in PV expression is observed in a particular brain region, it cannot be assumed that differences also exist in other brain regions. Therefore, systematic analyses are warranted. In some cases, changes in the number/distribution of PV⁺ cells in a particular brain region are correlated with altered electrophysiological properties. For example, in *Ambra1*^{+/-} mice, a likely reduction in PV—observed as a decrease in PV⁺ cell number and PV protein level and interpreted as a loss of hippocampal PV interneurons (Nobili et al., 2018)—was correlated with an overall reduction in inhibitory input from Pvalb neurons in CA1 pyramidal cells. Moreover, the perisomatic paired-pulse ratio (PPR) was increased in female *Ambra1*^{+/-} mice, which was also consistent with PV downregulation. These changes lead to hyperexcitability of CA1 pyramidal neurons and excitatory/inhibitory (E/I) imbalance (**Table 1**). Of note, similar findings were observed in *Ehmt1*^{+/-} mice—a model for delayed circuit maturation—evidenced by a reduced number of PV⁺ neurons at early age (PND14) in several cortical regions and characterized by impaired E/I balance (**Table 1**).

It is unclear whether the previously reported reduction in the number of PV⁺ neurons is due to an actual decrease in Pvalb neuron count or PV downregulation because either of these would result in a smaller number of identifiable PV⁺ cells. In Pvalb neurons with a low PV expression level (~10–20 μM in hippocampus; Eggermann and Jonas, 2012)—but also in those with moderate expression (~100 μM in cortex and striatum)—a reduction in PV level could result in some Pvalb neurons falling below the threshold of detection by PV IHC, and they would thus be considered negative for PV. For example, in *PV*^{+/-} mice in which PV and *Pvalb* mRNA expression levels are reduced by ~50% in the forebrain (Filice et al., 2018) and cerebellum

(Schwaller et al., 2004), the number of PV⁺ neurons quantified by stereological methods was decreased by ~25–30% in the SSC, mPFC, and striatum (Filice et al., 2016). As a rule of thumb, a decrease in PV protein expression by an average of ~50% results in 25–30% of Pvalb neurons expressing PV at a level below the threshold of detection by IHC. Importantly, unlike in humans, almost all prototypic Pvalb neurons [expressing γ-aminobutyric acid (GABA)] in the mouse brain are surrounded by PNNs, which can be detected based on the lectin-binding capacity of their glycan components by VVA or *Wisteria floribunda agglutinin* (WFA). In many brain regions, the overlap between PV⁺ and PNN⁺ neurons is >90% (Härtig et al., 1992). Therefore, the number of VVA⁺ cells is a realistic estimate for the number of Pvalb neurons in mice. In *PV*^{+/-} mice, the number of VVA⁺ cells was unaltered in all brain regions known to be associated with ASD—namely, SSC, mPFC, and striatum (Filice et al., 2016). Even in mice completely lacking PV (i.e., the number of PV⁺ cells was zero), the number of VVA⁺ neurons did not differ from that in WT mice. While there is a global reduction in PV expression in *PV*^{+/-} mice, in other ASD models, the decrease is brain region specific, yet the number of VAA⁺ neurons in these regions is unchanged. Reduced PV level and fewer PV⁺ neurons were observed in the SSC of *Shank1*^{-/-} (-30% PV⁺ cells) mice and in the striatum of *Shank3B*^{-/-} (-30%), *Cntnap2*^{-/-} (-30%), and *in utero* valproic acid (VPA)-treated (-15%) mice, suggesting that the striatum is a hotspot for the ASD-associated downregulation of PV. Notably, in the abovementioned mouse models, there are other brain regions with unaltered numbers of PV⁺ neurons (Schwaller, 2020), and the number of VVA⁺ cells is also unchanged. Moreover, in regions with a reduced number of PV⁺ neurons, *Pvalb* mRNA and PV protein expression levels were decreased by ~50% (or by ~30% in VPA mice). Thus, the *Shank1*^{-/-}, *Shank3B*^{-/-}, *Cntnap2*^{-/-}, VPA, and *PV*^{-/-} ASD mouse models are characterized by PV downregulation and not the loss of Pvalb neurons. However, such information is unavailable for most of the ASD mouse models listed in **Table 1**, in which a decrease in the number/density of PV⁺ neurons has been reported in most cases. Nonetheless, such information can provide mechanistic insights as a decreased number or functional impairment of Pvalb neurons due to a reduction in PV is expected to alter the functioning of the neuronal network in distinct ways.

Irrespective of the cause of the decreased number of PV⁺ neurons, the mouse models listed in **Table 1** exhibit changes at the level of electrophysiology and behavior. Notably, many of the genes listed in **Table 1** are associated with ASD and linked to E/I imbalance (Table 1 in Lee et al., 2017). Processes/mechanisms contributing to physiologic E/I balance include the development of excitatory and inhibitory synapses, neurotransmission, and synaptic plasticity comprising homeostatic plasticity, activation of signaling pathways (e.g., excitation–transcription coupling), and modulation of intrinsic excitability (Nelson and Valakh, 2015; Lee et al., 2017). The few models in which such changes in electrophysiological properties are directly attributable to a decrease in PV level are described in detail in *Acute Reduction in PV Expression Induces ASD-Like Behavior in Juvenile Mice, While Promoting PV Expression in PV*^{+/-} *Mice Attenuates*

TABLE 1 | Mouse models with evidence of parvalbumin (PV) alterations and associated changes in electrophysiology and occurrence of autism spectrum disorder (ASD)-like behavior.

Mouse model/ <i>Gene name</i> / <i>Protein name</i> SFARI classification	Type of PV alteration(s)/age of testing	Electrophysiological alteration(s) relevant to Pvalb neuron function	ASD-like behavioral impairments (core and comorbidity)
(A) GENETIC MODELS LISTED IN THE SFARI GENE DATABASE (https://gene.sfari.org/) (S, SYNDROMIC)			
Cntnap2 ^{-/-} Cntnap2 Contactin associated protein-like 2 SFARI 2 (S)	STRIATUM, CORTEX (Penagarikano et al., 2011; Vogt et al., 2018) Reduction in the number of PV ⁺ cells (P14 and P30) STRIATUM (Lauber et al., 2018) Reduction in the number of PV ⁺ cells and <i>Pvalb</i> mRNA, no change in the number of VVA ⁺ (Pvalb) neurons (P25)	HIPPOCAMPUS (Jurgensen and Castillo, 2015) Altered inhibition onto CA1 pyramidal neurons • Reduced amplitude of putative perisomatic-evoked IPSCs • Increase in the frequency of spontaneous AP-driven IPSCs SSC (Antoine et al., 2019) Reduced inhibition and (feebly) decreased excitation in L2/L3 pyramidal cells • Impairment in Pvalb neuron-mediated feedforward eIPSCs • Reduced spontaneous spiking frequency of mEPSCs and mIPSCs	Stereotypic motor movements and communication and social abnormalities. Hyperactivity to thermal sensory stimuli (Penagarikano et al., 2011)
Ehmt1 ^{+/-} Ehmt1 Euchromatic histone Methyltransferase 1 SFARI Gene Archive 3 (S)	AUDITORY CORTEX (AC) L2/3 and 4, SSC L2/3 and 4, VISUAL CORTEX (VC) L2/3 and 4 (Negwer et al., 2020) Delay of PV ⁺ neuron maturation in early (P14) sensory development, with layer- and region-specific variability later (P28, P56) AC: Decrease in PV ⁺ neurons in L2/3 and 4 at P14 only SSC: reduced number of PV ⁺ /VVA ⁺ neurons at all ages in L4 only VC: no differences in L2/3 at all ages; reduced number of PV ⁺ and PV ⁺ /VVA ⁺ in L4 at P14	HIPPOCAMPAL ACUTE SLICES (Frega et al., 2020) Impairment in inhibitory transmission • Strong reduction of mIPSC amplitude and frequency in CA1 pyramidal cells at P21 • Increased inhibitory PPR responses specifically at 50 ms ISI in CA1 pyramidal cells following stimulation in <i>stratum radiatum</i> (P21) • Hyperexcitability in CA1 hippocampal excitatory neurons • Results indicate that Ehmt1 plays a role in controlling E/I balance by regulating inhibitory inputs onto CA1 pyramidal cells AUDITORY CORTEX ACUTE SLICES (Negwer et al., 2020) • Reduced mIPSC frequency, NOT amplitude in auditory cortex L2/3 pyramidal cells at P14–16. • Increased inhibitory PPR responses at ISI of 50, 100, and 200 ms • Decreased release probability of GABA determined from a 10-Hz stimulus train	Reduced social play in juvenile (P30) male, but not in female mice Prolonged social approach in the social approach assay (3-chamber assay) observed in adult (3 months) male and female Ehmt1 ^{+/-} mice Delayed (males) or absent (females) preference for social novelty Hypergrooming and reduced exploration in the open field (Balemans et al., 2010)
En2 ^{-/-} En2 Engrailed 2 SFARI 3	HIPPOCAMPUS, SSC (Tripathi et al., 2009) Reduction in the number of PV ⁺ cells (3–5 months) TRN (Provenzano et al., 2020) Reduction of <i>Pvalb</i> mRNA (P30) Reduction in the number of PV ⁺ cells (6 weeks) VISUAL CORTEX (L2/3 and L5/6) (Pirone et al., 2020) Increase in the number of PV ⁺ cells (P30 and adult)	No electrophysiology at cellular level reported	Deficits in reciprocal social interactions as juveniles and adults (Brielmaier et al., 2012)
Fmr1 ^{-/-} Fmr1 Fragile X-mental retardation protein (FMRP) SFARI 3 (S)	SSC (Selby et al., 2007) Reduction in the number of PV ⁺ cells (12 months) DEVELOPING AUDITORY CORTEX (Wen et al., 2019) Reduction in the number of PV ⁺ cells (P14, P21, P30)	SSC (barrel cortex layer 4) (Gibson et al., 2008) Reduced feedback inhibition mediated by FS (Pvalb) neurons • Decreased EPSC frequency on FS (Pvalb) neurons • Normal feed-forward inhibition > no change in inhibitory drive • Excitatory neurons intrinsically more excitable > increased evoked AP firing rate during 600-ms current injection	ASD-like core symptoms of altered social interaction and repetitive behaviors, hyperactivity (Pietropaolo et al., 2011). Mental retardation, anxiety, increased incidence of epilepsy, auditory hypersensitivity (Chen and Toth, 2001; Frankland et al., 2004)

(Continued)

TABLE 1 | Continued

Mouse model/ <i>Gene name</i> /Protein name SFARI classification	Type of PV alteration(s)/age of testing	Electrophysiological alteration(s) relevant to Pvalb neuron function	ASD-like behavioral impairments (core and comorbidity)
(A) GENETIC MODELS LISTED IN THE SFARI GENE DATABASE (https://gene.sfari.org/) (S, SYNDROMIC)			
<i>Mecp2</i>^{-/-} <i>Mecp2</i> Methyl-CpG-binding Protein-2 SFARI 2 (S)	VISUAL CORTEX (V1) (Krishnan et al., 2015; Patrizi et al., 2019) Accelerated maturation of PV network (P14 and P30) HIPPOCAMPUS CA3 (Calfa et al., 2015) Density of PV ⁺ interneurons not altered in CA3 (P40–P60) VISUAL CORTEX (Durand et al., 2012) Increased <i>Pvalb</i> mRNA levels PV-hyperconnectivity > increased PV immunofluorescence intensity as consequence of increased neurite complexity (from P15 on; persistent also in adulthood)	HIPPOCAMPUS CA3 (Calfa et al., 2015) Weaker synaptic inhibition onto CA3 pyramidal neurons resulting in larger E/I ratio in CA3 pyramidal neurons <ul style="list-style-type: none"> • Smaller amplitude, but higher mIPSCs frequency in pyramidal neurons; larger amplitude, but lower frequency of mEPSCs • Smaller slope of input/output (I/O) relationship • Lower frequency of spontaneous APs from FS (Pvalb) neurons > smaller and less frequent mEPSCs onto CA3 fast-spiking basket cells VISUAL CORTEX (Durand et al., 2012) Reduction of pyramidal neuron and network activity <ul style="list-style-type: none"> • Stronger inhibition of pyramidal neurons caused by a hyperinnervation by PV-expressing interneurons > low spontaneous and evoked neuronal activity and a general silencing of cortical circuitry 	Ataxia, stereotyped behaviors, seizures, motor, sensory, memory, and social deficits (Chao et al., 2010; Ito-Ishida et al., 2015)
<i>Nlgn3</i>^{-/-} <i>Nlgn3</i> Neurologin 3 SFARI 2	SSC (Gogolla et al., 2009) “Patchy” PV ⁺ cells (2–3 months)	HIPPOCAMPUS CA2 (Modi et al., 2019) Increased neuronal excitability and reduced inhibition <ul style="list-style-type: none"> • Increased frequency of spontaneous EPSCs and decrease in frequency of spontaneous IPSCs in CA2 pyramidal cells • strong reduction of perisomatic inhibition mediated by CCK neurons HIPPOCAMPUS CA1 (Polepalli et al., 2017) Decrease in Pvalb interneuron inhibition <ul style="list-style-type: none"> • Significant reduction in facilitation of EPSCs and spiking in Pvalb neurons lacking Nlgn3 	Impaired social novelty and social memory, hyperactivity, repetitive behaviors (Tabuchi et al., 2007; Rothwell et al., 2014)
<i>Nlgn3</i> R451C Knock-in substitution of Arg ⁴⁵¹ to Cys <i>Nlgn3</i> Neurologin 3 SFARI 2	SSC (Speed et al., 2015) PV ⁺ cell number unchanged (P13–17)	SSC (barrel cortex) (Tabuchi et al., 2007; Speed et al., 2015) Increase in inhibitory synaptic transmission <ul style="list-style-type: none"> • Increase in spontaneous mIPSC frequency in L2/3 pyramidal neurons • Increased amplitude of evoked IPSCs in L2/3 pyramidal neurons Pvalb neuron–pyramidal cell synaptic connections NOT altered <ul style="list-style-type: none"> • Unitary IPSC₅/IPSC₁ ratio unchanged; paired whole-cell recordings between Pvalb neurons and pyramidal neurons HIPPOCAMPUS CA1 (Etherton et al., 2011) Increase in AMPA and NMDA receptor-mediated excitatory synaptic transmission <ul style="list-style-type: none"> • Increased fEPSP slope and spontaneous mEPSCs frequency Increased evoked synaptic strength at inhibitory synapses <ul style="list-style-type: none"> • Larger eIPSC amplitude in L2/3 pyramidal neurons mPFC (in vivo recordings) (Cao et al., 2018) Decreased excitability of FS interneurons and dysfunction of gamma oscillation <ul style="list-style-type: none"> • Reduced firing frequency recorded from FS interneurons 	Impaired social interaction behaviors and enhanced spatial learning (Tabuchi et al., 2007; Etherton et al., 2011)

(Continued)

TABLE 1 | Continued

Mouse model/ <i>Gene name</i> / <i>Protein name</i> SFARI classification	Type of PV alteration(s)/age of testing	Electrophysiological alteration(s) relevant to Pvalb neuron function	ASD-like behavioral impairments (core and comorbidity)
(A) GENETIC MODELS LISTED IN THE SFARI GENE DATABASE (https://gene.sfari.org/) (S, SYNDROMIC)			
Shank3^{-/-} Shank3 SH3 and multiple ankyrin repeat domains 3 SFARI 1 (S)	STRIATUM (Filice et al., 2016) Reduction in the number of PV ⁺ cells and <i>Pvalb</i> mRNA, no change in the number of VVA ⁺ (Pvalb) neurons (P25) INSULAR CORTEX (Gogolla et al., 2014) Diminished PV ⁺ puncta on pyramidal cells (P70–100)	CORTICOSTRIATAL ACUTE SLICES (Peca et al., 2011) Disruption of striatal glutamatergic signaling • Decreased corticostriatal population spike amplitude • Reduced frequency and amplitude of AMPA-mediated mEPSC in MSN SSC (Chen et al., 2020) Excitatory neuron hyperactivity and inhibitory neuron hypoactivity • <i>in vivo</i> population calcium imaging (basal recordings and after stimulation: vibrissae motion detection task)	Hypergrooming, social deficits, sensory hyperactivity (Peca et al., 2011; Chen et al., 2020)
(B) 'ENVIRONMENTAL' AND IDIOPATHIC MODELS			
VPA Environmental model of ASD (<i>in utero</i> exposure to valproic acid)	SSC (Gogolla et al., 2014) “Patchy” distribution of PV ⁺ cells (2–3 months) SSC, STRIATUM (Lauber et al., 2016) Reduction in the number of PV ⁺ cells and <i>Pvalb</i> mRNA, no change in VVA ⁺ (Pvalb) neurons (P25)	TEMPORAL CORTEX (Banerjee et al., 2013) mIPSC impairment • Reduced mIPSC frequency, but increased rise time and decay time in L2/3 pyramidal cells • Lower input/output response of evoked IPSCs	Reduced communication, social deficits, repetitive behavior, stimuli hypersensitivity (Schneider and Przewlocki, 2005; Markram et al., 2008; Gandal et al., 2010)
BTBR T⁺ Itpr3^{fl}/J (BTBR T⁺ tf/J) strain Idiopathic model of ASD This strain carries the mutations “a” (non-agouti; black and tan) “ <i>Itpr3^{fl}</i> ” (inositol 1,4,5-triphosphate receptor 3; tufted), and “T” (brachyury)	INSULAR CORTEX (Gogolla et al., 2014) Diminished PV ⁺ puncta on pyramidal cells (P70–100) ANTERIOR CINGULATE CORTEX (Stephenson et al., 2011) Reduction in PV ⁺ cells (8–10 weeks)	INSULAR CORTEX (Gogolla et al., 2014) Impaired multisensory integration—weakened inhibitory circuitry • Decreased mIPSCs frequency recorded in pyramidal cells	Social deficits, impairments in vocal communication, stereotypic, repetitive behaviors, exaggerated auditory responses at low-moderate tones (McFarlane et al., 2008; Scattoni et al., 2011; Gogolla et al., 2014)
(C) GENETIC NDD MODELS WITH A FEEBLER LINK TO PV AND ASD			
Ambra1^{+/-} (female mice) Ambra1 Activating molecule in Beclin1-regulated autophagy SFARI Gene Archive 5	HIPPOCAMPUS (Nobili et al., 2018) Reduction in the number of PV ⁺ cells and PV protein levels (2–3 months)	HIPPOCAMPUS (Nobili et al., 2018) Reduction of inhibitory drive on CA1 pyramidal neurons • Reduced amplitude of dendritic eIPSCs • Reduced amplitude of Pvalb neuron-mediated perisomatic eIPSCs	Sociability and communication deficits (Nobili et al., 2018)
Aspm¹⁻⁷ Aspm Abnormal spindle-like microcephaly associated	HIPPOCAMPUS, TRN (Garrett et al., 2020) Reduction in the number of PV ⁺ cells (23 weeks)	n/a	Impaired short- and long-term object recognition memory (Garrett et al., 2020)
PV-Lmo4^{-/-} Lmo4 deletion in Pvalb neurons Lmo4 LIM domain only	ANTERIOR CINGULATE CORTEX (Zhang et al., 2020a) No detectable loss of PV ⁺ neurons (2–4 months)	ANTERIOR CINGULATE CORTEX (ACC) L2/3 (Zhang et al., 2020a) Altered properties of Pvalb neurons • Increased membrane excitability and shortened latency to the first AP • Increased amplitude of spontaneous inhibitory inputs (mostly from Pvalb neurons) to the somata of ACC L2/3 pyramidal cells Increased Pvalb neuron-mediated perisomatic feedforward inhibition	Repetitive behaviors and deficits in social interaction (Zhang et al., 2020a)

Social Behavioral Impairment. Permanent changes in the firing properties of Pvalb neurons, their inputs, or their targets in ASD mouse models alter the steady-state equilibrium (i.e., E/I balance). It was initially proposed that an increase in the E/I ratio could be causally related to ASD (Rubenstein and Merzenich, 2003); however, it has since been demonstrated in many models that a homeostatic or maladaptive change in the E/I balance in either direction is a hallmark of ASD. The relative contribution of E/I imbalance to ASD can vary according to ASD risk/susceptibility gene mutation, brain region, specific features of synapses, and developmental time point. Even in mice harboring the same mutation, the E/I balance is differentially affected across neuron subpopulations. For example, mice carrying the neuroligin 3 mutation R451C (NL3^{R451C}) show an increase in inhibitory synaptic transmission in SSC pyramidal cells—that is, increases in spontaneous inhibitory postsynaptic current (sIPSC) and evoked (e)IPSC frequency (Tabuchi et al., 2007) leading to a lower E/I ratio. However, in CA1 pyramidal neurons of the same mice, excitatory transmission mediated by N-methyl-D-aspartate (NMDA)- and α -amino-3-hydroxy-5-methyl-4-isoxazolepropionic acid (AMPA)-type glutamate receptors is increased. As the former shows greater involvement, the NMDA/AMPA ratio as well as E/I ratio are increased. The increase in NMDA/AMPA ratio does not occur in layer 2/3 pyramidal neurons of the SSC (Etherton et al., 2011). In the hippocampal CA1 pyramidal cells of *Cntnap2*^{-/-} mice, putative perisomatic input (likely via the axon initial segment, soma, and proximal dendrites) and eIPSC amplitude are decreased, while miniature excitatory postsynaptic current (mEPSC) frequency and amplitude are unchanged (Jurgensen and Castillo, 2015). However, there is a trend toward a lower NMDA/AMPA ratio in *Cntnap2*^{-/-} mice. On the contrary, the frequency (but not amplitude) of spontaneous action potential (AP)-driven IPSC is increased in mutant mice, whereas mIPSC is unchanged (both in frequency and amplitude). Strongly reduced layer 4 stimulation-evoked feedforward inhibition (i.e., eIPSC) and a smaller decrease in feedforward excitation (i.e., evoked EPSC) onto layer 2/3 SSC pyramidal cells results in a higher E/I ratio in several ASD mouse models including *Cntnap2*^{-/-} and *Fmr1*^{Y/-} mice (Antoine et al., 2019). This only weakly affects spontaneous (basal) spiking in layer 2/3 pyramidal cells *in vitro*; however, the whisker-evoked firing rate of FSI (likely Pvalb neurons) is reduced in these two ASD models (Antoine et al., 2019). The above examples provide evidence that dysfunctional GABAergic transmission—often perisomatic inhibition by Pvalb basket cells—is a critical aspect of ASD. How the absence of PV is directly implicated in altered GABAergic transmission is discussed in *PV Affects Pvalb Neuron Targets and Inputs*.

Acute Reduction in PV Expression Induces ASD-Like Behavior in Juvenile Mice, While Promoting PV Expression in PV^{+/-} Mice Attenuates Social Behavioral Impairment

Based on findings from ASD patients and ASD animal models discussed in *Decreased Number of PV⁺ Neurons in Human ASD Postmortem Brains: Pvalb Neuron Loss vs. PV* and

Downregulation and Animal NDD Models of ASD With Reduced PV Expression and/or Decreased Number/Altered Distribution of PV⁺ Neurons, respectively, as well as our own *in vitro* studies (reviewed in Schwaller, 2020), we investigated the role of PV in the development of an ASD-like behavioral phenotype using genetically modified mice. Experimental approaches typically used to demonstrate causality between an experimental manipulation at the molecular or cellular level and higher-order brain function(s) (e.g., network activity or behavioral phenotype) are based on perturbation of the system. For instance, removing a component (e.g., a protein) hypothesized to be directly implicated in a behavior is predicted to lead to its appearance, whereas when the same component has lower abundance (e.g., in haploinsufficiency), upregulation to a normal level is expected to attenuate/alleviate the behavior (rescue experiment). There are several caveats to this concept. During the process of downregulation and/or reappearance of the investigated protein, additional adaptive, compensatory, or homeostatic changes may occur, likely over varying time scales and to different degrees. Nonetheless, the knockdown and rescue approaches have been successful in many instances, including in the field of ASD. Re-expression of *Shank3* in a *Shank3* conditional knock-in mouse model rescued social interaction deficits and attenuated repetitive grooming behavior in adult mice (Mei et al., 2016); early genetic restoration of WT *Shank3* in *Shank3*^{E13} mutant mice rescued the same deficits as well as those in locomotion and rearing (Jaramillo et al., 2020). In *MeCP2*-overexpressing mice, reducing *MeCP2* level (e.g., by antisense oligonucleotide treatment) reversed behavioral deficits associated with *MECP2* duplication syndrome (Sztainberg et al., 2015). Of note, null mutant *Shank3* and *Mecp2* mice are models for delayed and precocious circuit maturation during development, respectively, and especially for perisomatic Pvalb neuronal circuit function (Gogolla et al., 2014). Both mutants show impaired multisensory integration in the insular cortex, likely due to an E/I circuit imbalance skewed toward excitation (*Shank3*^{-/-}) or inhibition (*Mecp2*^{-/-}), respectively. This suggests that an optimal E/I circuit balance depends on precise Pvalb neuronal circuit function (Figure 7 in Gogolla et al., 2014). Alterations in the time course of network development/maturation—especially during critical periods of plasticity [postnatal days (PND) 5–15 in mice]—are thought to contribute to the appearance of ASD-like behavioral traits (Leblanc and Fagiolini, 2011).

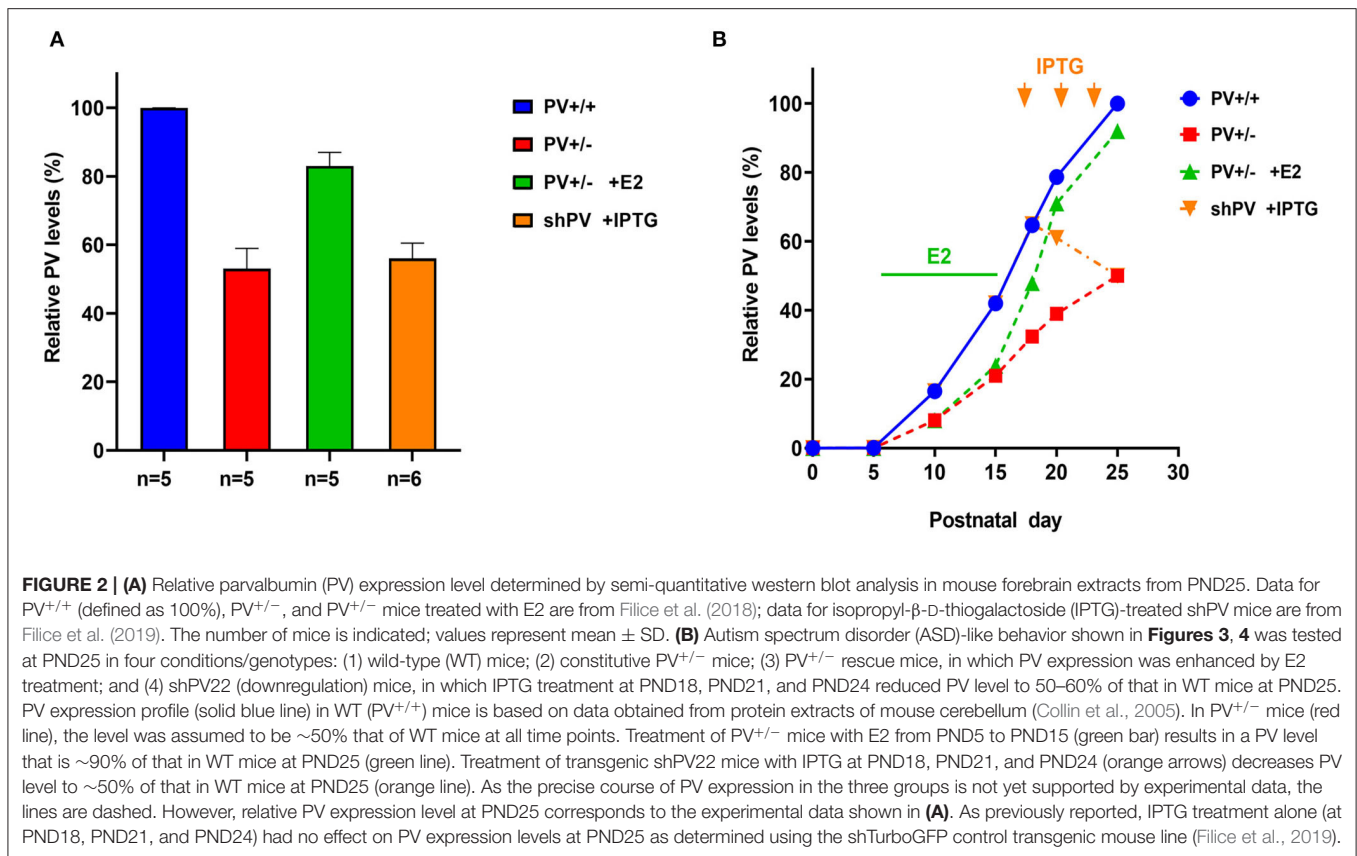
We applied the perturbation (removal/readdition) approach to investigate the role of PV in the occurrence of ASD-like core symptoms in mice. We previously showed that *PV*^{-/-} mice constitutively lacking PV expression exhibited all of the core ASD symptoms—i.e., reduced reciprocal social interaction, impaired communication (ultrasonic vocalization), and repetitive and stereotyped behaviors (Wöhr et al., 2015); they also showed several ASD-associated comorbidities such as increased susceptibility to epilepsy (Schwaller et al., 2004), reduced pain sensitivity (Wöhr et al., 2015), slight impairment of motor coordination, and mild hyperactivity (measured as characteristic speed) (Farre-Castany et al., 2007). The same but weaker core ASD-like phenotype is seen in *PV*^{+/-} mice (Wöhr et al., 2015), in which the level of PV is about 50% lower than

in WT mice (Schwaller et al., 2004; Filice et al., 2018). ASD-like behaviors in $PV^{-/-}$ and $PV^{+/-}$ mice have been consistently observed in the juvenile reciprocal social interaction assay and three-chamber assay evaluating direct social interaction and social preference, respectively. In the former, the most robust parameter distinguishing WT mice from those with reduced PV level ($PV^{+/-}$ and $PV^{-/-}$) was behavior following social behavior (Figure 3 legend and Figure 1D in Wöhr et al., 2015) and Figure 2C in Filice et al. (2018). In the three-chamber assay, the most relevant findings were related to sniff time—i.e., the time a mouse spent in close proximity (2 cm) to a caged stranger mouse – and not simply the time spent in the compartment with the stranger mouse; described in detail in the Supplementary Materials of Filice et al. (2018). To define the experimental conditions for the knockdown/rescue experiments, it is important to consider the developmental regulation of PV in Pvalb neurons. PV in mice is expressed starting from PND5 to PND7 (depending on the brain region), with peak expression occurring at approximately PND25–40 (Okaty et al., 2009). The developmental timeline of Pvalb neurons in the SSC (Figure 3 in Butt et al., 2017) and auditory cortex (Takesian et al., 2018) has been reported. An overview of cortical interneuron development can be found in Lim et al. (2018).

Quantitative data on PV expression levels during juvenile development in mice are available only for the cerebellum, which contains Purkinje cells and molecular layer interneurons (MLI) expressing PV (Figure 2B in Collin et al., 2005). These data were used to generate the blue curve for WT mice shown in **Figure 2B**. PV expression increases sharply starting at PND10 and reaches a plateau at PND20. The second postnatal week is also the start of the GABA switch from depolarizing to hyperpolarizing (observed in cultured hippocampal neurons) (Leonzino et al., 2016) that is essentially complete by PND12, as evidenced by the disappearance of giant depolarizing potentials (Ben-Ari et al., 1989; reviewed in Ben-Ari, 2002). Thus, the steep increase in PV expression begins at around the time when GABA action turns hyperpolarizing. The developmental course of PV expression may be different in other Pvalb neurons (in the cortex, hippocampus, and TRN). In $PV^{+/-}$ mice, we assumed the same temporal course as in WT mice; however, PV level reaching only 50% of WT at PND25 (Filice et al., 2018) (red curve in **Figure 2B**). For the rescue experiment, $PV^{+/-}$ mice were treated with 17- β -estradiol (E2) from PND5 to PND15, resulting in a PV expression level that was ~90% that of WT mice at PND25 (Filice et al., 2018). Hypothetical PV expression levels during the development of E2-treated mice are shown in **Figure 2B** (green curve). E2 has been shown to increase PV expression *in vitro* (Fujimoto et al., 2004) and in $PV^{+/-}$ mice (Filice et al., 2018); in the latter, this effect is mediated by an as-yet unidentified estrogen-responsive element (ERE) in the mouse *Pvalb* promoter. As E2 most likely affects the expression of several genes with identified EREs, what are the evidences that E2-mediated upregulation of PV is a most likely cause for the attenuation of the ASD-like phenotype in E2-treated $PV^{+/-}$ mice? Moreover, one has to take into account that E2 modulates social behavior in rats (Reilly et al., 2015) and more generally affects neural circuits via direct or

indirect activation of multiple downstream signaling pathways (Marino et al., 2006). First, in $PV^{-/-}$ mice, E2 had no obvious effect on PV expression or ASD-related behaviors (Filice et al., 2018). Second, although E2 treatment in WT mice does not increase global PV protein level, it is possible that PV protein is upregulated in some Pvalb neurons including those with low PV expression. Unexpectedly, E2 treatment provoked ASD-like behaviors in WT mice (e.g., decreased sociability and an increase in repetitive behavior). Possible reasons for this antisocial effect of E2 treatment in WT mice and additional arguments about the positive effect of E2 treatment selectively in $PV^{+/-}$ mice are discussed in Filice et al. (2018). Stronger PV IHC signals indicative of elevated PV level were also observed in $MeCP2^{-/-}$ ASD model mice (Patrizi et al., 2019), in accordance with the concept of optimal PV circuit function (Figure 7 in Gogolla et al., 2014). For the inverse experiment, we used the $B6PV^{Cre}$ -Tg(hPGK-eGFP/RNAi; Pvalb)^{1Swal} mouse line (abbreviated as shPV22 or shPV), which permits temporally controlled PV downregulation upon isopropyl- β -D-thiogalactoside (IPTG) administration (Filice et al., 2019). Induced expression of sh*Pvalb* from PND18 to PND25 decreased PV level to approximately 50–60% of the WT level (Filice et al., 2019), which was also comparable to the PV level in constitutive $PV^{+/-}$ mice. The hypothesized course of PV expression level is shown in **Figure 2B** (orange curve). It should be noted that the only experimentally verified PV levels in the rescue and downregulation experiments are those measured at PND25 (**Figure 2A**)—that is, the time point of behavioral testing; the green and orange curves in **Figure 2B** depicting PV expression levels in the two models are thus estimates that are not yet supported by experimental data.

ASD-like behavior was tested at PND25 for four conditions/genotypes: (1) WT; (2) constitutive $PV^{+/-}$; (3) $PV^{+/-}$ rescue, in which PV expression was enhanced by E2 treatment; and (4) shPV22 (downregulation), in which PV expression declined starting from PND18 to 50–60% at PND25. Results from the first three groups have been published (Wöhr et al., 2015; Filice et al., 2018), while behavioral data from shPV22 mice have not yet been reported. WT mice showed a strong preference (>60%) for engaging in another social behavior after a previous one (Wöhr et al., 2015; Filice et al., 2018) (**Figure 3**); this preference was not observed in $PV^{+/-}$ mice but was induced by increasing PV level through E2 treatment (Filice et al., 2018) and abolished after PV downregulation mediated by shPV22 starting from PND18. Almost identical results were observed in the three-chamber assay evaluating social preference: WT mice showed a stronger interest in the small cage with the stranger mouse than in the empty cage (object), as measured by sniff time (**Figure 4**). $PV^{+/-}$ mice showed no preference for the stranger mouse, but this was restored by E2-mediated PV upregulation. Transient PV reduction induced by IPTG in shPV22 mice attenuated preference for the stranger mouse compared to WT mice [$p = 0.024$ in the first cohort ($n = 6$) and $p = 0.179$ in the second cohort ($n = 4$)]. However, when results from the two cohorts were combined, a preference ($p = 0.0049$) for the stranger mouse is maintained—as to a lesser extent (n.s.)—in constitutive $PV^{+/-}$ mice (red and orange bars in **Figure 4**). In conclusion, induced downregulation of PV produces an



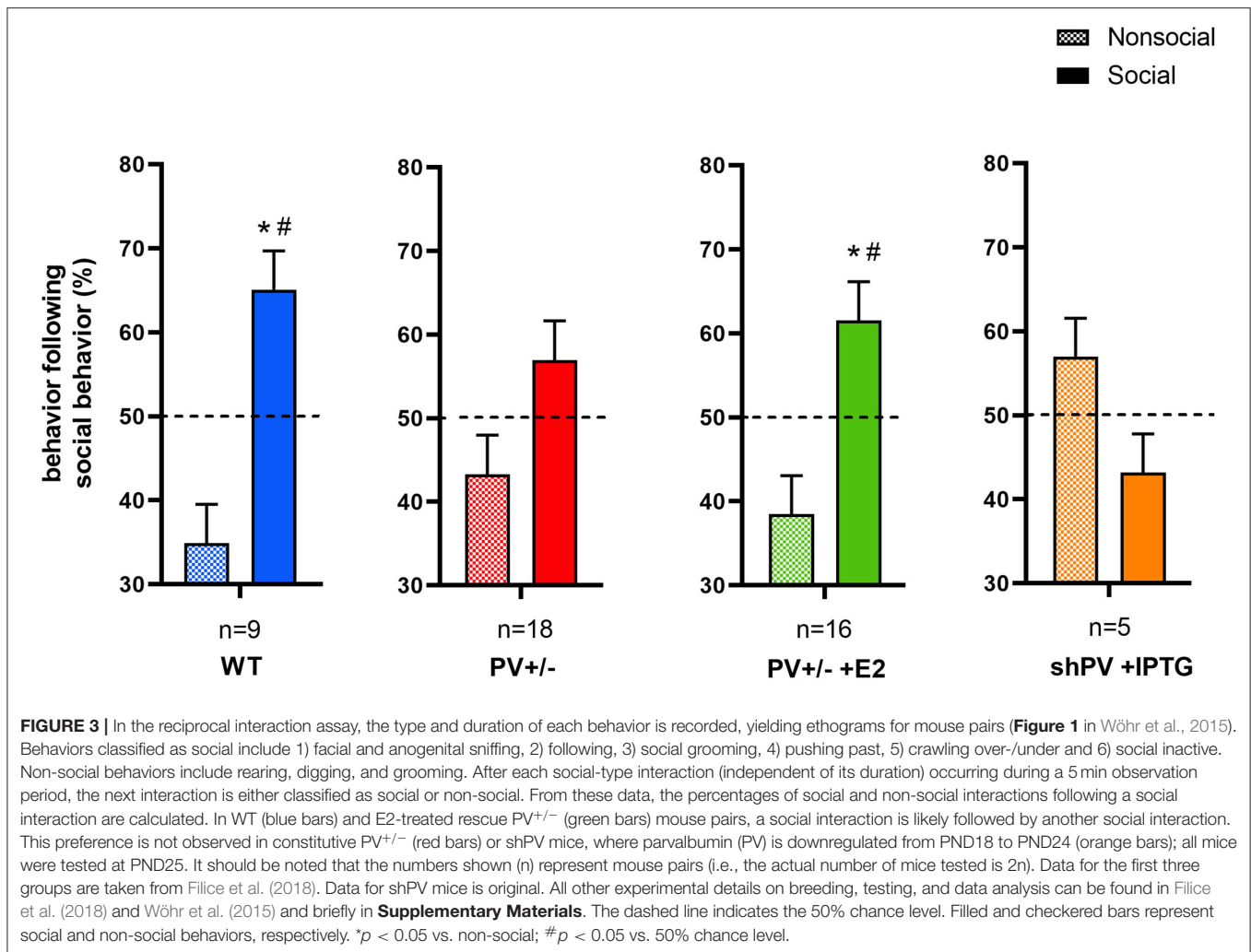
ASD-like phenotype, while PV restoration in constitutive PV^{+/-} mice abrogates this phenotype. This strongly indicates that PV expression level is causally related to ASD-like behavior. In the next sections, mechanistic and anatomic evidence supporting this possibility are presented.

PV Affects Pvalb Neuron Targets and Inputs

Biophysical Considerations

The function of an intracellular Ca²⁺ buffer (better termed as a Ca²⁺-signal modulator) like PV is simple in theory: binding Ca²⁺ ions at high intracellular Ca²⁺ concentration ([Ca²⁺]_i) and releasing/unbinding Ca²⁺ when local Ca²⁺ concentration decreases. PV-specific biophysical properties include Ca²⁺ as well as Mg²⁺ affinity and kinetics. Only the most pertinent findings are discussed here; additional details can be found in Schwaller (2020). Data on the biophysical properties of PV were obtained from *in vitro* studies using purified recombinant PV. Rat PV contains two equivalent Ca²⁺/Mg²⁺-binding sites that are usually occupied by either of the two ions in a competitive manner, with dissociation constants (K_D) of 11 nM and 41 μM, respectively (Eberhard and Erne, 1994). Modeling studies investigating the effect of PV on depolarization-induced increases in [Ca²⁺]_i in isolated chromaffin cells revealed physiologically relevant parameters including binding kinetics

(Lee et al., 2000) and apparent Ca²⁺ affinities (i.e., K_{D,Ca[app]} values of 150–250 nM in an intracellular environment). Together with PV mobility determined in neuron somata [diffusion rate (D_{PV}), ~40 μm² s⁻¹; Table 1 in Schwaller (2020)], these parameters should enable accurate prediction of the effect of a given concentration of PV on Ca²⁺ signals in a particular neuron if all other parameters relevant to Ca²⁺ signaling are known, such as the “on” mechanisms that lead to an increase in [Ca²⁺]_i as well as the “off” mechanisms that reduce [Ca²⁺]_i to basal levels (Berridge et al., 2003). However, such information is currently unavailable for essentially all proteins—for example, for a single voltage-gated Ca²⁺ channel Cav2.1 (P/Q type; *CACNA1A*) or a plasma membrane calcium ATPase (e.g., *PMCA1*; *ATP2B1*) many splice variants exist, exhibiting distinct properties related to Ca²⁺ handling. All of these Ca²⁺ signaling components are present to varying degrees in different neuron subpopulations (some highly specific and others ubiquitous); even in supposedly homogeneous subpopulations such as cerebellar MLIs, PV expression levels vary considerably among individual neurons [average ~570 μM; range, 55–1,788 μM (Eggermann and Jonas, 2012)]. Moreover, average PV concentrations in Pvalb neuron populations in different brain regions are highly heterogeneous, ranging from 10 μM in the hippocampus to ~750 μM in TRN (Janickova et al., 2020). To further complicate matters, organelles previously assumed to be homogeneous such as mitochondria that are



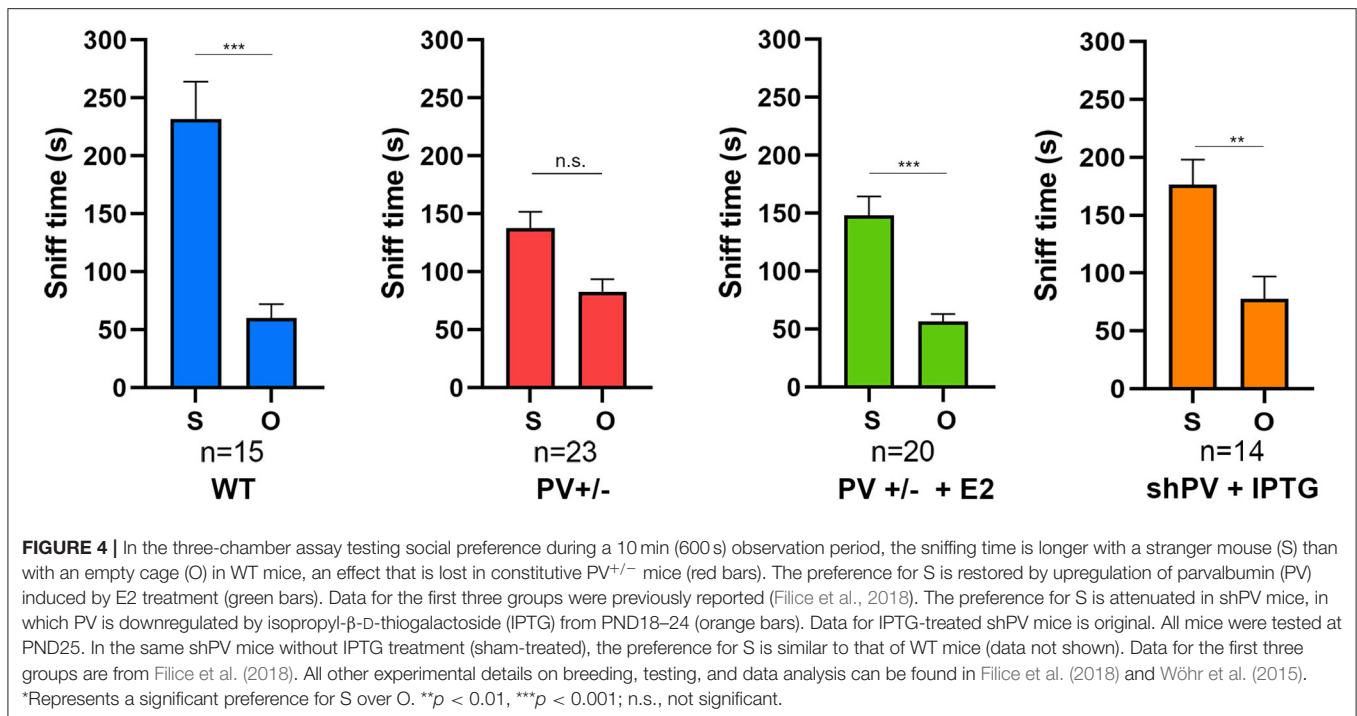
also involved in Ca²⁺ signaling/sequestration—especially in (pre)synaptic compartments (Devine and Kittler, 2018)—express a highly diverse set of proteins implicated in mitochondrial Ca²⁺ transport (Fecher et al., 2019), which is discussed in detail in *Effect of PV on Mitochondria, Oxidative Stress, and Pvalb Neuron Morphology: Link to NDDs*. Despite the complexity of the experimental data, certain global principles of neuronal Ca²⁺ signaling have been deduced.

The slow Ca²⁺-binding kinetics of PV generally exclude an effect on the fast-rising phase of Ca²⁺ transients, for instance those elicited by the opening of voltage- or receptor-operated Ca²⁺ channels such as Ca_v2.1 (*CACNA1A*) or NMDA-type glutamate receptor (e.g., *GRIN1*). The same holds true for depolarization-evoked increases in [Ca²⁺]_i in PV-loaded chromaffin cells (Figure 7 in Lee et al., 2000). PV accelerates the initial rate of [Ca²⁺]_i decay, often transforming a monoexponential decay into a biexponential one with fast and slow decay components (τ_{fast} and τ_{slow} , respectively) (Collin et al., 2005; Muller et al., 2007). This property of PV prevents/delays the gradual buildup of presynaptic [Ca²⁺]_i (e.g., within a train of APs) that subsequently affects short-term modulation of synaptic

plasticity. This has been observed in a model system based on PV-loaded chromaffin cells (Lee et al., 2000). The following aspects of PV function can be understood from this model: (1) buildup of residual [Ca²⁺]_i is delayed but not prevented; (2) the effect of PV is dependent on the time interval between stimuli and is strongest at the time point when the [Ca²⁺]_i decay curve with or without PV shows the largest difference; (3) if stimuli are long enough [i.e., all PV molecules are loaded with Ca²⁺ (last part of the rising phase in Figure 7 in Lee et al., 2000)], the maximum amplitude of the Ca²⁺ signal is independent of PV; and (4) [Ca²⁺]_i decay following such a train is slowed/prolonged by Ca²⁺-loaded PV acting as a Ca²⁺ source (“on” mechanism). Evidence for a direct role of PV under these conditions is summarized below, although only a few selected examples are discussed; additional details can be found in the chapter on PV in Schwaller (2020).

Effect of PV on Synaptic Transmission

Higher residual Ca²⁺ in the absence of PV is the likely reason for increased paired-pulse facilitation (PPF) at the synapses between MLI and Purkinje cells (Caillard et al., 2000), hippocampal Pvalb neurons and CA1 pyramidal cells (Vreugdenhil et al., 2003),



striatal Pvalb neurons and medium spiny neurons (MSN) (Orduz et al., 2013), and at the calyx of Held, a glutamatergic synapse (Muller et al., 2007). The last of these examples is an exception, as most Pvalb neurons are GABAergic; nonetheless, it demonstrates that the inhibitory effect of PV on PPF is independent of neurotransmitter type. The prevention (reduction) of facilitation is a hallmark of PV. The PV-mediated effect size on PPF depends on many parameters but most importantly on PV concentration, stimulation frequency [interspike interval (ISI)], number of spikes, and Ca²⁺ on/off kinetics in Pvalb neurons. The role of PV as a delayed Ca²⁺ source has been investigated in less detail, although delayed release at GABAergic synapses has been observed (Lu and Trussell, 2000; Kirischuk and Grantyn, 2003). At MLI-MLI synapses, an MLI firing in bursts (10 APs) induces long-lasting asynchronous release for up to 2,400 ms after the train; the duration is much shorter (400 ms) in PV^{-/-} MLIs (Collin et al., 2005). Interestingly, the IPSC integral of the delayed release in WT MLIs is greater than that of the signal generated during the AP train. Thus, the synaptic output of MLIs is random and almost constant during the interburst period; the mean signal intensity is essentially determined by the number of APs in the preceding burst. In summary, MLIs (and likely other Pvalb neurons, e.g., in the cortex) alternately adopt a phasic signaling mode during bursts and an integrating (tonic) signaling mode between bursts (Collin et al., 2005). PV has a different effect on sustained asynchronous release by layer 5 Pvalb neuron autapses in the SSC (Manseau et al., 2010). In the absence of PV, asynchronous release from the autaptic terminal is slightly but significantly increased; this decreases Pvalb neuron spike reliability and reduces the ability of pyramidal neurons to integrate incoming stimuli to

produce precise firing. As each Pvalb neuron innervates multiple pyramidal neurons, asynchronous release from a single one may desynchronize a large portion of the local network and disrupt cortical information processing. While Pvalb autapses have been implicated in precise spike timing (required, for example, for synchronous oscillations) (Deleuze et al., 2019), asynchronous release reduces the spike precision and reliability of cortical neurons and thereby disrupts synchronous firing when the activity level surpasses a threshold value in order to prevent/decrease the generalized synchronous activity observed during epileptic discharges (Manseau et al., 2010). In the absence of PV (i.e., with increased asynchronous release), the onset of pentylenetetrazole-induced tonic-clonic seizures was found to be delayed in PV^{-/-} mice, although the intensity of the subsequent generalized seizures was higher (Schwaller et al., 2004).

Yet another effect of PV may contribute to the modulation of intracellular Ca²⁺ signaling, especially in Pvalb neurons with high, near-millimolar PV concentrations such as MLIs (Eggermann and Jonas, 2012) and TRN neurons (Janickova et al., 2020). In these neurons, the large pool of Mg²⁺-bound PV does not usually slow the effective Ca²⁺-binding rate but instead contributes to the regeneration of metal-free (apo) PV that acts as a fast Ca²⁺ buffer. Therefore, Mg²⁺ binding/unbinding may serve as a metabuffering (buffering of buffering) mechanism that maintains the concentration of apo-PV during rapid, repetitive activity in fast-spiking Pvalb neurons (Eggermann and Jonas, 2012; Hu et al., 2014). While proteins including Kv3.1b are a prerequisite for the fast afterhyperpolarization that characterizes Pvalb neurons, extracellular matrix molecules of the mostly negatively charged PNN components contribute to their rapid firing. PNNs are thought to establish local molecular gradients of

physiologically relevant ions such as Ca^{2+} , K^+ , or Na^+ around Pvalb neuron somata (Morawski et al., 2015). Accordingly, treatment with chondroitinase ABC—a bacterial enzyme that cleaves polysaccharide chains of PNN components—significantly (~50%) decreased Pvalb neuron firing frequency in cortical slices (Tewari et al., 2018).

PV influences spike reliability through asynchronous release and also during bursting activity. Besides the expected effect of increasing PPF at striatal Pvalb neuron–MSN synapses, the absence of PV leads to increased Pvalb neuron excitability and more regular spontaneous spiking within a train. Experimental (Orduz et al., 2013) and modeling (Bischof et al., 2012) data indicate that the likely cause of the latter is a change in the activation of small conductance (SK) Ca^{2+} -dependent K^+ channels. Thus, the presence of PV at the synapse induces arrhythmicity (i.e., increase in “jitter”) by modulating intrinsic oscillations via SK channel activation (Orduz et al., 2013). The triad of SK channels, voltage-dependent Ca^{2+} channels, and sarco(endoplasmic) reticulum Ca^{2+} ATPase (SERCA) pumps enables the generation of Ca^{2+} signaling-dependent oscillatory activity in the TRN (Cueni et al., 2008); in striatal Pvalb neurons and likely in TRN Pvalb neurons, PV is a fourth component that contributes to this process by increasing the irregularity of the oscillatory spiking pattern (Orduz et al., 2013). How the absence of PV affects TRN Pvalb neuron function *in vivo* is discussed in *Striatum and TRN as a Hub in NDDs: Role of Pvalb Neurons*.

Functional phenotypes observed in $\text{PV}^{-/-}$ mice related to excitability, synaptic transmission, short-term modulation, firing properties, and network effects (e.g., oscillations) may represent the extreme end of decreased PV-induced changes because reduced but not complete loss of PV expression is usually observed in human NDDs and corresponding animal models. The functional consequences of a direct or indirect (i.e., secondary to NDD risk gene mutations) decrease in PV level are discussed here. A small hairpin (sh)RNA was used to assess the role of PV in cortical circuits of adolescent rats (PND34–38) (Caballero et al., 2020). PV level in the PFC was decreased by ~25% at PND65, resembling the NDD rodent phenotype of lower PV expression at an older age (>PND60). In layer 5 pyramidal cells, the frequency of sIPSCs was reduced and PV deficiency was observed, which increased facilitation (i.e., a higher PPF ratio at an ISI of 50 ms). As sEPSC frequency was unchanged, the reduction in PV led to an increase in the E/I ratio in pyramidal cells. On the contrary, the frequency of sEPSCs was decreased in fast-spiking cortical Pvalb neurons. Hippocampal-evoked local field potential (LFP) responses in the PFC are affected by a lower PV level in a frequency-dependent manner: at 20 and 40 Hz, LFP facilitation occurs while control rats show LFP depression. In summary, higher PV expression is required for refinement of prefrontal GABAergic function, while its absence results in immature afferent processing and a hypofunctional state (Caballero et al., 2020).

Results from the above-described study cannot be directly compared to experiments carried out in $\text{PV}^{+/-}$ mice. Unlike in PV-shRNA rats, no data are available from $\text{PV}^{+/-}$ mice on LFPs in the PFC *in vivo* or IPSCs mediated by fast-spiking (Pvalb) neurons and EPSCs determined *ex vivo*. Moreover,

behavioral data from PV-shRNA rats are sparse. In the trace fear conditioning and extinction test, acquisition of a cue-mediated fear response was unaffected by a reduction in PV level, while fear extinction was prolonged. Compared to controls, PV-shRNA rats showed increased freezing times lasting until the last trial of cue presentation (Caballero et al., 2020). Similar findings were obtained in the reward-based T-maze reversal learning assay carried out in $\text{PV}^{-/-}$ mice to assess behavioral inflexibility: while the initial learning phase was identical for WT and $\text{PV}^{-/-}$ mice, a large proportion of the latter exhibited a clear deficit in the ability to reverse their behavior in order to receive the reward (Wöhr et al., 2015). It will be interesting to determine whether PV-shRNA rats also exhibit repetitive and stereotyped ASD-like behaviors. Additionally, electrophysiological recordings of the PFC in $\text{PV}^{+/-}$ mice may reveal similarities between the two models in terms of neuronal firing properties and behavior.

Alterations in Synaptic Transmission in NDD Mouse Models Suggest PV Involvement

Mice lacking the ASD-associated gene *LMO4* (encoding an endogenous inhibitor of PTP1B phosphatase) specifically in Pvalb neurons [*PV-Lmo4* knockout (KO) mice] show increased Pvalb neuron-mediated perisomatic feedforward inhibition (likely by basket cells) onto pyramidal cells (Zhang et al., 2020a), as well as increased excitability of Pvalb neurons in the dorsal anterior cingulate cortex (dACC). Spontaneous inhibitory inputs (sIPSC amplitude) mostly from Pvalb neurons onto dACC layer 2/3 pyramidal cells are increased while excitatory inputs are less affected, resulting in a lower E/I ratio. Optogenetically induced activation of Pvalb neurons was shown to increase PPF. Differences between WT and KO mice were greatest at an ISI of around 20–50 ms, while short-term depression of IPSCs in a train (e.g., at 20 Hz) was reduced in KO mice. The broadened AP signal in *PV-Lmo4* KO mice may be attributable to a reduction in delayed rectifying potassium conductance (by $\text{K}_V1.2$ or K_V3) (Zhang et al., 2020a). Given the close association (coexpression) of PV and $\text{K}_V3.1b$ in most cortical Pvalb neurons (Chow et al., 1999), a decrease in $\text{K}_V3.1b$ is a potential mechanism for AP broadening. It is worth noting that, at the behavioral level, *PV-Lmo4* KO mice display typical ASD core symptoms of reduced social interaction and repetitive, stereotyped behaviors (Table 1).

As discussed above and shown in Table 1, PV expression is altered in several genetic and “environmental” mouse ASD models (*Animal NDD Models of ASD With Reduced PV Expression and/or Decreased Number/Altered Distribution of PV⁺ Neurons*). Changes in proteins involved in synaptic transmission have been reported in these mice and are briefly summarized here. The level of *Kcnc1* transcript encoding the $\text{K}_V3.1b$ channel necessary for maintaining the fast-spiking phenotype of Pvalb neurons was decreased slightly in $\text{PV}^{-/-}$ mouse and significantly (–40%) in VPA mouse forebrain lysates (including neocortex, thalamus, and pallidus) (Lauber et al., 2016). The latter mice are characterized by reduced PV expression in the striatum (Lauber et al., 2016). In the cortex, $\text{K}_V3.1b$ shows near-perfect overlap with PV (99% of all PV^+ neurons are $\text{K}_V3.1b^+$ and vice versa) (Du et al., 1996; Chow et al., 1999; Lien and Jonas, 2003). The expression and function of hyperpolarization-activated cyclic

nucleotide-gated (HCN) channels responsible for I_h currents are important for regulating resting membrane potential, input resistance, dendritic integration, synaptic transmission, and neuronal excitability (Biel et al., 2009; Benarroch, 2013). These channels are altered in ASD mouse models, often in those with decreased PV expression. This is the case for *Shank3B*^{-/-} mice expressing a lower level of PV in striatal Pvalb neurons (Filice et al., 2016). Cultures of developing hippocampal neurons derived from these mice show increased input resistance and excitability as well as drastically attenuated I_h currents and reduced expression of *Hcn4* protein (Yi et al., 2016). Reduced *Hcn4* mRNA and PV levels are also seen in the striatum of *Cntnap2*^{-/-} mice (Laubert et al., 2018). Moreover, *Hcn1* mRNA expression in the striatum was decreased slightly in *PV*^{-/-} and significantly in *Shank3B*^{-/-} mice at PND25 (Laubert et al., 2016). On the contrary, *Hcn1* mRNA and HCN1 protein levels were elevated (by ~40%) in the forebrain of PND25 VPA mice that showed no difference in forebrain PV expression relative to the control (Laubert et al., 2016). Thus, brain region- and gene-specific (*Gad1*, *Pvalb*, *Kcnc1*, *Hcn1-4*, and *Kcnn1-4*) alterations may be responsible for (maladaptive) homeostatic mechanisms and are observed in several ASD models, mostly those with decreased PV level; some of these are likely cell autonomous and linked to Pvalb neuron hypofunction (e.g., *Gad1*, *Pvalb*, and *Kcnc1*), as are the downstream consequences of reduced (absent) PV expression such as increases in the number of mitochondria and dendritic branching (as discussed in *Effect of PV on Mitochondria, Oxidative Stress, and Pvalb Neuron Morphology: Link to NDDs*). Altered expression of HCN family members *Hcn1-4* or potassium calcium-activated channel subfamily N members 1–4 (SK channels) that are not specifically expressed in or even absent from Pvalb neurons reflect a Pvalb neuronal circuit phenotype caused by PV downregulation-mediated functional changes in Pvalb neurons. However, the putative changes (e.g., alterations in neuronal activity of one neuron subpopulation leading to parallel or hierarchical changes in others) have not been fully elucidated.

Adding yet another level of complexity, the absence of PV in striatal PV neurons has a presumed retrograde effect on the cortical glutamatergic inputs onto Pvalb neurons. In the time window (10–50 ms) when Pvalb neuron–MSN synapses show stronger facilitation in the absence of PV, PPF of EPSCs between cortical neurons and striatal Pvalb neurons—mostly mediated by AMPA receptors—is significantly reduced (Wöhr et al., 2015). The same effect is observed in *PV*^{+/-} mice, in which a ~50% reduction in PV level was sufficient to influence PPF at this corticostriatal synapse. Further experiments have suggested that changes in short-term plasticity at the cortical neuron–FSI synapse involve a presynaptic adaptation mechanism, possibly resulting from homeostatic plasticity in the cortical neuron caused by the absence/reduction in PV in the postsynaptic striatal Pvalb neuron. However, the lack of a direct link (synapse) between Pvalb neurons and their cortical inputs indicate a retrograde or circuit (network) effect. In summary, the removal/decrease in PV in Pvalb neurons has complex effects on intracellular Ca^{2+} signaling and synaptic transmission even without considering the changes induced at the morphological

level (discussed in *Effect of PV on Mitochondria, Oxidative Stress, and Pvalb Neuron Morphology: Link to NDDs*).

Striatum and TRN as a Hub in NDDs: Role of Pvalb Neurons

Several brain regions and associated circuits have been investigated in the context of NDDs including the basal ganglia and thalamus, and especially the TRN. The basal ganglia are involved in motor learning, habit formation, and stimulus processing to generate appropriate responses; they are also implicated in mood, motivation, and decision making (goal-directed action). These processes involve the cortico–basal ganglia–thalamocortical loop in which cortical pyramidal cells project to the striatum, with striatal neurons giving rise to direct and indirect pathways. In the former, the neurons project to the internal segment of the globus pallidus, which sends efferents to the thalamus; projections from the thalamus to the cortex close the loop. In the indirect pathway, a fiber bundle from the striatum reaches the external segment of the external globus pallidus, which forms synapses with neurons of the subthalamic nucleus (STN). The STN projects to the thalamus and from there back to the cortex. The term “disclosed loop” has been used to describe a closed circuit that is open to outside influence at the initial stage of cortical input (Figure 8 in Shipp, 2017). Patients with a damaged striatum often show autistic traits (Damasio and Maurer, 1978; Maurer and Damasio, 1982) and stereotyped movements. In male mice, dorsal striatum-specific damage (by coablation of ~40–50% Pvalb neurons and large cholinergic interneurons) results in spontaneous stereotypy and deficits in social interaction (Rapanelli et al., 2017). Restricted and repetitive behaviors are also linked to alterations in striatal and thalamic circuits (Farmer et al., 2013). Functional brain imaging studies have revealed the involvement of corticostriatal–thalamic circuits in ASD (Fuccillo, 2016), and morphological studies of the thalamus and striatum indicate differences such as a larger volume (Schuetze et al., 2016) and surface area and greater rostrocaudal variation in the shape of the thalamus in ASD patients compared to control subjects (Schuetze et al., 2019). ASD rodent models with striatal and thalamic alterations have been developed to investigate the mechanisms underlying such dysfunctions. Details on the striatal impairment in these mutant mice can be found in Table 1 of Li and Pozzo-Miller (2019).

Mutations in several ASD-associated genes affect corticostriatal connectivity (reviewed in Fuccillo, 2016; Li and Pozzo-Miller, 2019) or general striatal structure or function as observed in human ASD patients (Langen et al., 2007; Estes et al., 2011) and multiple ASD mouse models such as *Fmr1*^{-/-} (Centonze et al., 2008), *Shank3*^{-/-} (Peca et al., 2011), *Cntnap2*^{-/-} (Penagarikano et al., 2011), and *Cntnap4*^{-/-} (Karayannis et al., 2014). Another possible feature of corticostriatal dysfunction in ASD is abnormalities in Pvalb neurons, including decreased PV expression in striatal Pvalb neurons likely caused by mutations in ASD risk genes such as *CNTNAP2* and *SHANK3* (Table 1).

Although Pvalb neurons account for just 1% of striatal neurons (Tepper et al., 2010), they are responsible for ~10%

of all striatal activity (Duhne et al., 2020). Striatal Pvalb neurons receive projections from different cortical regions (mainly primary motor cortex and primary SSC) as well as inhibitory input from TRN (Klug et al., 2018), which is often described as the “guardian of the gateway” (Crick, 1984), and selectively modulates the thalamocortical network, playing a critical role in sensorimotor and cognitive functions, sleep, and consciousness (Crick, 1984; Schmitt et al., 2017). It is unsurprising that abnormalities in the thalamocortical circuitry are associated with some of the sensory perceptual deficits typical of ASD; thus, TRN dysfunction is considered as a prototypical circuit endophenotype in NDDs (Krol et al., 2018). NDD risk genes associated with schizophrenia (*CACNA1I* and *GRM3*) and ASD (*CHD2* and *PTCHD1*) are strongly expressed in TRN, and as they are also thought to be linked to Pvalb neurons, results obtained in the mutant mice are discussed here. TRN neurons comprise two (mainly non-overlapping) populations characterized by expression of either PV (~60% of neurons) or SST (~40%) (Clemente-Perez et al., 2017; Steullet et al., 2017a). The cell types differ in terms of intrinsic membrane excitability and low-threshold Ca^{2+} current (I_T) mediated by $Ca_v3.2$ and $Ca_v3.3$ (Talley et al., 1999). Peak I_T density is higher in Pvalb neurons, suggesting that SST neurons have fewer and/or more dendritically located T-type calcium channels (Clemente-Perez et al., 2017). Hyperpolarization of TRN neurons leads to low-threshold Ca^{2+} spikes in the form of rebound bursts, each crowned by a series of APs. The maximal number of rebound bursts, number of APs after the first burst, and intraburst frequency are higher in Pvalb neurons than in SST cells (Clemente-Perez et al., 2017). $Ca_v3.3$ channels are required for TRN cell bursting and synchronized rhythmicity in the thalamic circuit. Absence of $Ca_v3.3$ channels (*Cacna1i*) in $Ca_v3.3^{-/-}$ mice decreases I_T by ~80% and almost completely abolishes the bursting properties of TRN neurons (that likely express Pvalb) (Astori et al., 2011). A lack of $Ca_v3.3$ channels also reduces apamin-sensitive currents mediated by SK2 channels, indicating that $Ca_v3.3$ /SK2 channel interactions are required for the proper functioning of the latter in TRN neurons (Cueni et al., 2008). Interestingly, KO mouse models of ASD and schizophrenia have shown similar findings with respect to TRN neuron function both *in vivo* and in slice cultures.

In vivo recordings of TRN Pvalb neurons in anesthetized $PV^{-/-}$ mice have revealed altered proportions of neurons with specific firing properties: medium-bursting (type II) neurons were more abundant than the long-bursting type (III), indicating a decrease in rebound bursting in the absence of PV. Additionally, the ISI within a burst was longer, while the number of spikes was unaffected (Alberi et al., 2013). These changes are likely associated with an altered distribution of $Ca_v3.2$ channels mediating I_T . $Ca_v3.2$ channels are more abundant at active axosomatic synapses of $PV^{-/-}$ TRN neurons as compared to WT TRN neurons, suggesting that the differential localization of $Ca_v3.2$ affects bursting dynamics. Notably, the distribution of $Ca_v3.3$ channels is similar in the two genotypes. TRN neurons express apamin-sensitive SK channels (Cueni et al., 2008), and the absence of PV is therefore presumed to have a similar effect on TRN neuron SK currents as in the striatum (Orduz et al., 2013).

A cross-correlation analysis of neurons simultaneously recorded with the same electrode tip showed that ~30% of neuron pairs tended to fire synchronously independent of PV expression. Hence, PV deficiency does not affect the functional connectivity between TRN neurons that are also coupled by chemical synapses (Zhang et al., 2020b), as is the case in cortical Pvalb neurons (Galarreta and Hestrin, 1999), but affects the distribution of $Ca_v3.2$ channels and dynamics of burst discharges in TRN cells, possibly by modulating SK channel activity. Other KO mouse models of Ca^{2+} signaling components (e.g., the schizophrenia risk gene *Disc1*) show a strong effect on the function of TRN neurons, which most likely involves SK channels (Delevich et al., 2020). In mice, patch-domain containing protein 1 (PTCHD1) is expressed almost exclusively in TRN neurons at PND0 and is still prominently expressed at PND15. *Ptchd1*^{Y/-} mice with TRN neuron-specific deletion of the ASD- and intellectual disability-associated *Ptchd1* gene showed attention deficit and hyperactivity along with a 50% reduction in SK currents, which were rescued by a pharmacological treatment that restored SK channel function (Wells et al., 2016). Importantly, at all investigated membrane potentials of *Ptchd1*^{Y/-} TRN neurons in cultured slices, the number of rebound bursts was smaller than in WT mice, whereas no difference was observed in I_T . Thus, the reduced bursting activity of *Ptchd1*^{Y/-} TRN neurons is likely the result of decreased SK currents. Moreover, free $[Ca^{2+}]_i$ is significantly lower in *Ptchd1*^{Y/-} TRN neurons, providing further evidence of altered intracellular Ca^{2+} handling.

Effect of PV on Mitochondria, Oxidative Stress, and Pvalb Neuron Morphology: Link to NDDs

The two major roles of mitochondria are the generation of ATP via oxidative phosphorylation and Ca^{2+} buffering. In neurons, these two processes occur not only globally but also locally—for example, in presynapses (reviewed in Devine and Kittler, 2018). The electrophysiological properties of Pvalb neurons require both fast presynaptic Ca^{2+} handling and sufficient energy production to sustain high-frequency firing. PV is a component of the Ca^{2+} signaling toolkit involved in the regulation of intracellular $[Ca^{2+}]_i$ (Berridge et al., 2003). A high firing rate of cortical GABAergic interneurons including Pvalb neurons is observed *in vivo*, which is more physiologically relevant than the fast-firing properties of Pvalb neurons that were mostly measured *in vitro*. Two-photon *in vivo* calcium imaging in the SSC of mice has revealed that GABAergic interneurons have higher activity than excitatory neurons, measured as event rate using the Ca^{2+} indicator GCaMP6 expressed in either neuron population (Chen et al., 2020). PV acting as a slow-onset Ca^{2+} buffer mostly serves as a “ Ca^{2+} off” mechanism that reduces $[Ca^{2+}]_i$ after an initial increase in conjunction with two other essential “ Ca^{2+} off” components—namely, SERCA pumps and PMCAs—that require ATP for this function. How the absence or partial downregulation of PV affects a cell expressing PV under physiological conditions remains an open question. A Ca^{2+} overlay blot with protein extracts of forebrain and cerebellum did not show upregulation of EF-hand Ca^{2+} -binding proteins similar to PV in the brain

of PV^{-/-} mice (Schmidt et al., 2003). On the other hand, fast-twitch muscles of PV^{-/-} mice are more resistant to fatigue as a result of increased fractional volume (density) of mitochondria (Chen et al., 2001). This inverse (antagonistic) regulation (i.e., PV downregulation and overexpression increasing and decreasing mitochondrial volume, respectively) occurs in all systems investigated to date including tissues/cells endogenously expressing PV such as fast-twitch muscle cells, kidney epithelial cells, and Pvalb neurons (Schwaller, 2020). The same mechanism exists in cells overexpressing PV including neurons of Thy-PV mice (Van Den Bosch et al., 2002; Maetzler et al., 2004), C2C12 muscle cells (Ducreux et al., 2012), MDCK kidney epithelial cells (Henzi and Schwaller, 2015), and CG4 oligodendrocyte-like cells (Lichvarova et al., 2019). Mitochondria are functionally similar to PV in terms of shaping intracellular Ca²⁺ transients: neither greatly affects the rising phase because of their slow-onset Ca²⁺-buffering/Ca²⁺-uptake properties but increases the rate of [Ca²⁺]_i decay, thus shortening Ca²⁺ transients, and both have anti-facilitating effects at presynaptic terminals—i.e., they accelerate recovery from synaptic depression (e.g., in the calyx of Held; Kim et al., 2005), thereby participating in the clearance of presynaptic Ca²⁺ and modulating neurotransmitter release (Billups and Forsythe, 2002). According to the notion of activity-dependent homeostatic changes/adaptations (Berridge et al., 2003), mitochondria are in the best position (with respect to Ca²⁺ signal modulation) to compensate for a loss/decrease in PV. Moreover, while SERCA pumps and PMCAs are not obviously upregulated in PV-deficient cells, they are presumed to contribute more extensively to Ca²⁺ removal in the absence of PV (although this has yet to be demonstrated). Thus, PV-deficient Pvalb neurons likely need to produce more ATP to accommodate the increased activity of Ca²⁺ extrusion systems. Ca²⁺ uptake by mitochondria is energetically costly and can only be maintained by increasing ATP production (Palmieri and Persico, 2010). Conversely, Ca²⁺ buffering by PV is an energy-saving process, as the small conformational changes in PV induced by Ca²⁺ binding/Ca²⁺ release require little energy and are independent of ATP levels.

Mitochondria were previously assumed to be homogeneous in terms of composition and function but are now known to be highly diverse within different organs (Mootha et al., 2003) and even in different cells of the brain, as demonstrated in cerebellar granule cells, Purkinje cells, and astrocytes (Fecher et al., 2019). This is also true of cell components involved in Ca²⁺ signaling, which show cell-type specific regulation (Fecher et al., 2019). Several experimental models with reduced PV expression show not only an increased mitochondrial volume but also elevated levels of mitochondrial proteins directly related to Ca²⁺ uptake. In epithelial cells of the distal convoluted tubule in mouse kidney, several genes implicated in mitochondrial Ca²⁺ uptake and generation of mitochondrial membrane potential including mitochondrial calcium uptake 1 (*Micu1*), mitochondrial calcium uniporter regulator 1 (*Mcur1*), and mitochondrial cytochrome c oxidase subunit 1 (*mt-Co1*) are upregulated in PV^{-/-} mice (Henzi and Schwaller, 2015). Levels of *COXI* and positive regulators of mitochondria biogenesis (*Ppargc1a*, *Nrf1*, and *Tfam*) are higher in PV-negative CG4 cells than in those

overexpressing PV (Lichvarova et al., 2019). However, no differences are observed in the expression of mitochondrial genes directly linked to ATP synthesis such as F1-ATPase subunit (*Atp5F1b*) (reviewed in Schwaller, 2020), further suggesting that the increases in mitochondrial volume and protein expression likely enhance the slow Ca²⁺-buffering capacity conferred by PV in WT cells. Additionally, transcript levels of mitochondrial uncoupler protein UCP2 (*Ucp2*) are elevated in control (PV⁻) CG4 cells (similar to the condition in PV^{-/-} mice) compared to PV-expressing CG4 cells (mimicking the condition in WT Pvalb neurons) (L. Janickova, unpublished). This is in line with RNA-seq results from cortical samples of ASD patients demonstrating that *UCP2* is among the most strongly upregulated transcripts (Parikshak et al., 2016; Schwede et al., 2018). Consistent with findings from PV^{-/-} mice, transcript levels of several genes related to synaptic transmission and mitochondria are altered in ASD (Schwede et al., 2018), and expression-weighted cell type enrichment analysis of three mouse ASD and schizophrenia models revealed significant upregulation of mitochondrial genes in fast-firing inhibitory (presumably Pvalb) neurons, while mitochondrial protein levels showed a global downregulation in the cortex (Gordon et al., 2019).

The increase in the density of mitochondria is not homogeneous in the soma of Pvalb neurons and is mostly observed in the region adjacent to the plasma membrane in Purkinje cells (Chen et al., 2006) as well as in striatal and TRN Pvalb neurons (Janickova and Schwaller, 2020). Previously, it was unclear whether this is an on/off or precisely regulated mechanism. Analyses of nine different Pvalb neuron populations from five different brain regions (hippocampus, cortex, striatum, cerebellum, and TRN) selected based on moderate-to-strong PV staining revealed a strong positive correlation between the magnitude of the increase in mitochondrial density and estimated PV concentrations in Pvalb neurons of WT mice—i.e., a higher PV concentration was associated with a greater PV deficiency-induced increase in mitochondrial density (but not in the length of individual mitochondria). Such an increase exists not only in PV^{-/-} Pvalb neuron somata but also in the dendrites (Janickova et al., 2020), confirming an earlier finding that mitochondrial density was higher in control CG4 (PV⁻) cells than in those overexpressing PV (Lichvarova et al., 2019). In particular, more mitochondria are present at the end of elongating processes and near the growth cone in control CG4 cells, which likely promotes process branching similar to what is observed in PV^{-/-} striatal and TRN Pvalb neurons (Janickova et al., 2020). Whether increased dendrite length and branching in the absence of PV results in local hyperconnectivity as observed in several ASD mouse models (Table 1 in Janickova et al., 2020) remains to be determined. More detailed information on mitochondria and branching can be found in the Discussion of Janickova et al. (2020).

The fast-firing property of Pvalb neurons is associated with their high energy demand (Kann et al., 2014; Kann et al., 2014); accordingly, Pvalb neurons contain significantly more mitochondria in their somata, dendrites, and axons than any other interneuron subtype or pyramidal cells. This makes Pvalb neurons especially vulnerable to metabolic stress and/or excessive

formation of reactive oxygen and nitrogen species (ROS and NOS, respectively) (Kann, 2016). ROS production increases with age in Pvalb neurons of WT mice and is highly correlated with PV concentration but not mitochondrial density, which is similar (~8%) in all investigated Pvalb neurons (Janickova and Schwaller, 2020); that is, between the ages of 1 and 6 months, a higher PV concentration is associated with an age-dependent increase in ROS production. Importantly, in the absence of PV, ROS production is significantly higher in mice older than 1 month and the relative increase is approximately proportional to the PV concentration in WT Pvalb neurons (Janickova and Schwaller, 2020). An elevation in ROS levels causing an imbalance in redox homeostasis has been suggested as a pathophysiological mechanism of ASD (Tang et al., 2013; Pangrazzi et al., 2020). Increased ROS levels have also been observed in postmortem brain tissue of children with ASD (Siddiqui et al., 2016).

Increased mitochondrial ROS production and Pvalb neuron impairment (possibly linked to decreased PV level) have been causally linked to schizophrenia etiology and pathology (reviewed in Hardingham and Do, 2016; Steullet et al., 2016, 2017b). In *Gclm*^{-/-} mice—a schizophrenia mouse model deficient in the glutamate cysteine ligase modifier subunit, the rate-limiting enzyme for glutathione biosynthesis (Cabungcal et al., 2019)—the number of PV⁺/PNN⁺ neurons is decreased. This may be due to Pvalb neuron loss or a decrease in PV expression and altered molecular composition of PNNs, possibly as a result of neuron immaturity (Steullet et al., 2017a). In brain slices from *Gclm*^{-/-} mice, most TRN neurons were shown to fire in a tonic mode at a membrane potential of -70 mV, whereas ~80% neurons in WT mice exhibit bursting behavior. At more negative membrane potentials (-80 and -90 mV), no differences in bursting behavior existed between genotypes. While membrane potential-dependent differences in firing behavior of TRN neurons are correlated with decreased PV level in *Gclm*^{-/-} TRN neurons, a causal relationship between these events has yet to be established. Notably, a decrease in the number of PV⁺ neurons in the TRN has been reported in other ASD models showing behavioral phenotypes such as the *Engrailed-2* KO mice (*En2*^{-/-}) and abnormal spindle-like microcephaly-associated gene (*Aspm1-7*) mutants (Garrett et al., 2020; Pirone et al., 2020). Whether this is due to PV downregulation—and the electrophysiological consequences thereof—remains unclear.

Brain-development-dependent mitochondrial alterations (dysfunction) may trigger a cascade of events that leads to NDDs such as ASD or schizophrenia (Tang et al., 2013; Cabungcal et al., 2019). However, at least in 1 month-old PV^{-/-} mice showing no increase in ROS production (Janickova and Schwaller, 2020) but exhibiting robust ASD-like behaviors, excessive oxidative stress can be excluded as the main contributor to the ASD phenotype. The onset of oxidative-stress-induced Pvalb neuron dysfunction may occur at a later age and result in a schizophrenia-like rather than an ASD-like phenotype, although this is speculative and must be tested in longitudinal studies using different NDD mouse models. Supporting the oxidative stress hypothesis of NDD, inhibiting oxidative stress in schizophrenia patients

by treatment with the antioxidant N-acetyl-cysteine (NAC) significantly improved neurocognition and alleviated positive clinical symptoms (Klauser et al., 2018; Retsa et al., 2018). However, in young individuals with ASD, NAC treatment for 12 weeks boosted glutathione production but did not improve social interaction deficits (Wink et al., 2016). Meanwhile, symptoms of irritability were attenuated in children with ASD who were treated with NAC (Hardan et al., 2012). Additional studies are required to determine whether NAC can reduce ASD core symptoms.

CONCLUSIONS AND OUTLOOK

We have formulated the Parvalbumin Hypothesis of ASD based on experimental data (new and previously published) (**Figure 1**). This hypothesis pertaining to the etiology of ASD (and possibly schizophrenia) provides a framework for future research and allows the formulation of predictions that can be tested in human ASD postmortem brain samples or using the many existing animal models of ASD. This hypothesis does not hold true for all ASD cases and may even be restricted to a small number of cases with known genetic mutations or environmental perturbations in which downregulation of PV has been reported. The validation of a hub consisting of PV-expressing neurons in ASD is expected to facilitate the development of therapeutic strategies that restore brain function(s) in ASD and possibly other NDDs.

DATA AVAILABILITY STATEMENT

The raw data of novel experiments described in the article supporting the conclusions of this article will be made available by the authors, without undue reservation.

ETHICS STATEMENT

The animal study was reviewed and approved by the Cantonal Veterinary Office (Canton of Fribourg, Switzerland). Experiments were performed according to institutional guidelines of the present Swiss law and the European Communities Council Directive of 24 November 1986 (86/609/EEC). The authorization number for housing of mice is H-04.2012-Fr and for the experiments 2016_37_FR and 2019_24_FR.

AUTHOR CONTRIBUTIONS

FF, LJ, TH, AB, and BS contributed to data collection (literature research). FF, TH, and AB carried out the experiments and performed data analysis. BS conceived the concept of the article. All authors were involved in writing the paper and read and approved the final manuscript.

FUNDING

The experimental part of this study was supported by a Simons Foundation Autism Research Initiative (SFARI) Explorer award

(# 603695) to BS and by the Swiss National Science Foundation SNF grants # 155952 and 184668 to BS.

ACKNOWLEDGMENTS

We thank all investigators and collaborators in the many research labs (>35) worldwide (>10 countries) with whom we have had the privilege of collaborating and publishing many findings on the role of PV in the last two decades. The integration of results obtained in different transgenic mouse lines, various tissues and organs (brain, fast-twitch muscle, and kidney), and in cell-based systems allowed us to develop the

Parvalbumin Hypothesis of ASD. Additionally, we thank Simone Eichenberger, Natascha Bersier, and Marie Bardet (University of Fribourg) for assistance in maintaining the mouse facility and Valerie Salicio, Marlene Sanchez, and Anne Oberson for technical assistance.

SUPPLEMENTARY MATERIAL

The Supplementary Material for this article can be found online at: <https://www.frontiersin.org/articles/10.3389/fncel.2020.577525/full#supplementary-material>

REFERENCES

- Alberi, L., Lintas, A., Kretz, R., Schwaller, B., and Villa, A. E. (2013). The calcium-binding protein parvalbumin modulates the firing properties of the reticular thalamic nucleus bursting neurons. *J. Neurophysiol.* 109, 2827–2841. doi: 10.1152/jn.00375.2012
- Antoine, M. W., Langberg, T., Schnepel, P., and Feldman, D. E. (2019). Increased excitation-inhibition ratio stabilizes synapse and circuit excitability in four autism mouse models. *Neuron* 101, 648–661.e644. doi: 10.1016/j.neuron.2018.12.026
- Ariza, J., Rogers, H., Hashemi, E., Noctor, S. C., and Martinez-Cerdeno, V. (2018). The number of chandelier and basket cells are differentially decreased in prefrontal cortex in autism. *Cereb. Cortex* 28, 411–420. doi: 10.1093/cercor/bhw349
- Astori, S., Wimmer, R. D., Prosser, H. M., Corti, C., Corsi, M., Liaudet, N., et al. (2011). The Ca(V)3.3 calcium channel is the major sleep spindle pacemaker in thalamus. *Proc. Natl. Acad. Sci. U. S. A.* 108, 13823–13828. doi: 10.1073/pnas.1105115108
- Balemans, M. C. M., Huibers, M. M. H., Eikelenboom, N. W. D., Kuipers, A. J., Van Summeren, R. C. J., Pijpers, M. M. C. A., et al. (2010). Reduced exploration, increased anxiety, and altered social behavior: autistic-like features of euchromatin histone methyltransferase 1 heterozygous knockout mice. *Behav. Brain Res.* 208, 47–55. doi: 10.1016/j.bbr.2009.11.008
- Banerjee, A., Garcia-Oscos, F., Roychowdhury, S., Galindo, L. C., Hall, S., Kilgard, M. P., et al. (2013). Impairment of cortical GABAergic synaptic transmission in an environmental rat model of autism. *Int. J. Neuropsychopharmacol.* 16, 1309–1318. doi: 10.1017/S1461145712001216
- Bayer, K. U., and Schulman, H. (2019). CaM kinase: still inspiring at 40. *Neuron* 103, 380–394. doi: 10.1016/j.neuron.2019.05.033
- Ben-Ari, Y. (2002). Excitatory actions of GABA during development: the nature of the nurture. *Nat. Rev. Neurosci.* 3, 728–739. doi: 10.1038/nrn920
- Ben-Ari, Y., Cherubini, E., Corradetti, R., and Gaiarsa, J. L. (1989). Giant synaptic potentials in immature rat CA3 hippocampal neurones. *J. Physiol.* 416, 303–325. doi: 10.1113/jphysiol.1989.sp017762
- Benarroch, E. E. (2013). HCN channels: function and clinical implications. *Neurology* 80, 304–310. doi: 10.1212/WNL.0b013e31827dec42
- Berridge, M. J., Bootman, M. D., and Roderick, H. L. (2003). Calcium signalling: dynamics, homeostasis and remodelling. *Nat. Rev. Mol. Cell Biol.* 4, 517–529. doi: 10.1038/nrm1155
- Biel, M., Wahl-Schott, C., Michalakakis, S., and Zong, X. (2009). Hyperpolarization-activated cation channels: from genes to function. *Physiol. Rev.* 89, 847–885. doi: 10.1152/physrev.00029.2008
- Billups, B., and Forsythe, I. D. (2002). Presynaptic mitochondrial calcium sequestration influences transmission at mammalian central synapses. *J. Neurosci.* 22, 5840–5847. doi: 10.1523/JNEUROSCI.22-14-05840.2002
- Bischoff, D. P., Orduz, D., Lambot, L., Schiffmann, S. N., and Gall, D. (2012). Control of neuronal excitability by calcium binding proteins: a new mathematical model for striatal fast-spiking interneurons. *Front. Mol. Neurosci.* 5:78. doi: 10.3389/fnmol.2012.00078
- Briellmaier, J., Matteson, P. G., Silverman, J. L., Senerth, J. M., Kelly, S., Genestine, M., et al. (2012). Autism-relevant social abnormalities and cognitive deficits in engrailed-2 knockout mice. *PLoS ONE* 7:e40914. doi: 10.1371/journal.pone.0040914
- Butt, S. J., Stacey, J. A., Teramoto, Y., and Vagnoni, C. (2017). A role for GABAergic interneuron diversity in circuit development and plasticity of the neonatal cerebral cortex. *Curr. Opin. Neurobiol.* 43, 149–155. doi: 10.1016/j.conb.2017.03.011
- Caballero, A., Flores-Barrera, E., Thomases, D. R., and Tseng, K. Y. (2020). Downregulation of parvalbumin expression in the prefrontal cortex during adolescence causes enduring prefrontal disinhibition in adulthood. *Neuropsychopharmacology* 45, 1527–1535. doi: 10.1038/s41386-020-0709-9
- Cabungcal, J. H., Steullet, P., Kraftsik, R., Cuenod, M., and Do, K. Q. (2019). A developmental redox dysregulation leads to spatio-temporal deficit of parvalbumin neuron circuitry in a schizophrenia mouse model. *Schizophr. Res.* 213, 96–106. doi: 10.1016/j.schres.2019.02.017
- Caillard, O., Moreno, H., Schwaller, B., Llano, I., Celio, M. R., and Marty, A. (2000). Role of the calcium-binding protein parvalbumin in short-term synaptic plasticity. *Proc. Natl. Acad. Sci. U. S. A.* 97, 13372–13377. doi: 10.1073/pnas.230362997
- Calfa, G., Li, W., Rutherford, J. M., and Pozzo-Miller, L. (2015). Excitation/inhibition imbalance and impaired synaptic inhibition in hippocampal area CA3 of Mecp2 knockout mice. *Hippocampus* 25, 159–168. doi: 10.1002/hipo.22360
- Cao, W., Lin, S., Xia, Q. Q., Du, Y. L., Yang, Q., Zhang, M. Y., et al. (2018). Gamma oscillation dysfunction in mPFC leads to social deficits in neuroigin 3 R451C knockin mice. *Neuron* 97, 1253–1260.e1257. doi: 10.1016/j.neuron.2018.02.001
- Celio, M. R. (1990). Calbindin D-28k and parvalbumin in the rat nervous system. *Neuroscience* 35, 375–475. doi: 10.1016/0306-4522(90)90091-H
- Celio, M. R., Spreafico, R., de Biasi, S., and Vitellaro-Zuccarello, L. (1998). Perineuronal nets: past and present. *Trends Neurosci.* 21, 510–515. doi: 10.1016/S0166-2236(98)01298-3
- Centonze, D., Rossi, S., Mercaldo, V., Napoli, I., Ciotti, M. T., De Chiara, V., et al. (2008). Abnormal striatal GABA transmission in the mouse model for the fragile X syndrome. *Biol. Psychiatry* 63, 963–973. doi: 10.1016/j.biopsych.2007.09.008
- Chao, H. T., Chen, H., Samaco, R. C., Xue, M., Chahrouh, M., Yoo, J., et al. (2010). Dysfunction in GABA signalling mediates autism-like stereotypies and Rett syndrome phenotypes. *Nature* 468, 263–269. doi: 10.1038/nature09582
- Chen, G., Carroll, S., Racay, P., Dick, J., Pette, D., Traub, I., et al. (2001). Deficiency in parvalbumin increases fatigue resistance in fast-twitch muscle and upregulates mitochondria. *Am. J. Physiol. Cell Physiol.* 281, C114–122. doi: 10.1152/ajpcell.2001.281.1.C114
- Chen, G., Racay, P., Bichet, S., Celio, M. R., Egli, P., and Schwaller, B. (2006). Deficiency in parvalbumin, but not in calbindin D-28k upregulates mitochondrial volume and decreases smooth endoplasmic reticulum surface selectively in a peripheral, subplasmalemmal region in the soma of Purkinje cells. *Neuroscience* 142, 97–105. doi: 10.1016/j.neuroscience.2006.06.008

- Chen, L., and Toth, M. (2001). Fragile X mice develop sensory hyperreactivity to auditory stimuli. *Neuroscience* 103, 1043–1050. doi: 10.1016/S0306-4522(01)00036-7
- Chen, Q., Deister, C. A., Gao, X., Guo, B., Lynn-Jones, T., Chen, N., et al. (2020). Dysfunction of cortical GABAergic neurons leads to sensory hyperreactivity in a Shank3 mouse model of ASD. *Nat. Neurosci.* 23, 520–532. doi: 10.1038/s41593-020-0598-6
- Chow, A., Erisir, A., Farb, C., Nadal, M. S., Ozaita, A., Lau, D., et al. (1999). K(+) channel expression distinguishes subpopulations of parvalbumin- and somatostatin-containing neocortical interneurons. *J. Neurosci.* 19, 9332–9345. doi: 10.1523/JNEUROSCI.19-21-09332.1999
- Chow, M. L., Pramparo, T., Winn, M. E., Barnes, C. C., Li, H. R., Weiss, L., et al. (2012). Age-dependent brain gene expression and copy number anomalies in autism suggest distinct pathological processes at young versus mature ages. *PLoS Genet.* 8:e1002592. doi: 10.1371/journal.pgen.1002592
- Clemente-Perez, A., Makinson, S. R., Higashikubo, B., Brovarney, S., Cho, F. S., Urry, A., et al. (2017). Distinct thalamic reticular cell types differentially modulate normal and pathological cortical rhythms. *Cell Rep* 19, 2130–2142. doi: 10.1016/j.celrep.2017.05.044
- Cohen, S. M., Ma, H., Kuchibhotla, K. V., Watson, B. O., Buzsaki, G., Froemke, R. C., et al. (2016). Excitation-transcription coupling in parvalbumin-positive interneurons employs a novel CaM kinase-dependent pathway distinct from excitatory neurons. *Neuron* 90, 292–307. doi: 10.1016/j.neuron.2016.03.001
- Collin, T., Chat, M., Lucas, M. G., Moreno, H., Racay, P., Schwaller, B., et al. (2005). Developmental changes in parvalbumin regulate presynaptic Ca²⁺ signaling. *J. Neurosci.* 25, 96–107. doi: 10.1523/JNEUROSCI.3748-04.2005
- Crick, F. (1984). Function of the thalamic reticular complex: the searchlight hypothesis. *Proc. Natl. Acad. Sci. U. S. A.* 81, 4586–4590. doi: 10.1073/pnas.81.14.4586
- Cueni, L., Canepari, M., Lujan, R., Emmenegger, Y., Watanabe, M., Bond, C. T., et al. (2008). T-type Ca²⁺ channels, SK2 channels and SERCAs gate sleep-related oscillations in thalamic dendrites. *Nat. Neurosci.* 11, 683–692. doi: 10.1038/nn.2124
- Damasio, A. R., and Maurer, R. G. (1978). A neurological model for childhood autism. *Arch. Neurol.* 35, 777–786. doi: 10.1001/archneur.1978.00500360001001
- Deleuze, C., Bhumra, G. S., Pazienti, A., Lourenco, J., Mailhes, C., Aguirre, A., et al. (2019). Strong preference for autaptic self-connectivity of neocortical PV interneurons facilitates their tuning to gamma-oscillations. *PLoS Biol.* 17:e3000419. doi: 10.1371/journal.pbio.3000419
- Delevich, K., Jaaro-Peled, H., Penzo, M., Sawa, A., and Li, B. (2020). Parvalbumin interneuron dysfunction in a thalamo-prefrontal cortical circuit in *discl* locus impairment mice. *eNeuro* 7:ENEURO.0496-19.2020. doi: 10.1523/ENEURO.0496-19.2020
- Devine, M. J., and Kittler, J. T. (2018). Mitochondria at the neuronal presynapse in health and disease. *Nat. Rev. Neurosci.* 19, 63–80. doi: 10.1038/nrn.2017.170
- Du, J., Zhang, L., Weiser, M., Rudy, B., and Mcbain, C. J. (1996). Developmental expression and functional characterization of the potassium-channel subunit Kv3.1b in parvalbumin-containing interneurons of the rat hippocampus. *J. Neurosci.* 16, 506–518. doi: 10.1523/JNEUROSCI.16-02-00506.1996
- Ducreux, S., Gregory, P., and Schwaller, B. (2012). Inverse regulation of mitochondrial volume and the cytosolic Ca²⁺ buffer parvalbumin in muscle cells via SIRT-1/PGC-1 α axis. *PLoS ONE* 7:e44837. doi: 10.1371/journal.pone.0044837
- Duhne, M., Lara-Gonzalez, E., Laville, A., Padilla-Orozco, M., Avila-Cascajares, F., Arias-Garcia, M., et al. (2020). Activation of parvalbumin-expressing neurons reconfigures neuronal ensembles in murine striatal microcircuits. *Eur. J. Neurosci.* 1–16. doi: 10.1111/ejn.14670
- Durand, S., Patrizi, A., Quast, K. B., Hachigian, L., Pavlyuk, R., Saxena, A., et al. (2012). NMDA receptor regulation prevents regression of visual cortical function in the absence of Mecp2. *Neuron* 76, 1078–1090. doi: 10.1016/j.neuron.2012.12.004
- Eberhard, M., and Erne, P. (1994). Calcium and magnesium binding to rat parvalbumin. *Eur. J. Biochem.* 222, 21–26. doi: 10.1111/j.1432-1033.1994.tb18836.x
- Ebert, D. H., and Greenberg, M. E. (2013). Activity-dependent neuronal signalling and autism spectrum disorder. *Nature* 493, 327–337. doi: 10.1038/nature11860
- Eggermann, E., and Jonas, P. (2012). How the 'slow' Ca²⁺ buffer parvalbumin affects transmitter release in nanodomain-coupling regimes. *Nat. Neurosci.* 15, 20–22. doi: 10.1038/nn.3002
- Estes, A., Shaw, D. W., Sparks, B. F., Friedman, S., Giedd, J. N., Dawson, G., et al. (2011). Basal ganglia morphometry and repetitive behavior in young children with autism spectrum disorder. *Autism Res.* 4, 212–220. doi: 10.1002/aur.193
- Etherton, M., Foldy, C., Sharma, M., Tabuchi, K., Liu, X., Shamloo, M., et al. (2011). Autism-linked neuroligin-3 R451C mutation differentially alters hippocampal and cortical synaptic function. *Proc. Natl. Acad. Sci. U. S. A.* 108, 13764–13769. doi: 10.1073/pnas.1111093108
- Farmer, C., Thurm, A., and Grant, P. (2013). Pharmacotherapy for the core symptoms in autistic disorder: current status of the research. *Drugs* 73, 303–314. doi: 10.1007/s40265-013-0021-7
- Farre-Castany, M. A., Schwaller, B., Gregory, P., Barski, J., Mariethoz, C., Eriksson, J. L., et al. (2007). Differences in locomotor behavior revealed in mice deficient for the calcium-binding proteins parvalbumin, calbindin D-28k or both. *Behav. Brain Res.* 178, 250–261. doi: 10.1016/j.bbr.2007.01.002
- Fecher, C., Trovo, L., Muller, S. A., Snaidero, N., Wettmarshausen, J., Heink, S., et al. (2019). Cell-type-specific profiling of brain mitochondria reveals functional and molecular diversity. *Nat. Neurosci.* 22, 1731–1742. doi: 10.1038/s41593-019-0479-z
- Ferguson, B. R., and Gao, W. J. (2018). PV interneurons: critical regulators of e/i balance for prefrontal cortex-dependent behavior and psychiatric disorders. *Front. Neural Circuits* 12:37. doi: 10.3389/fncir.2018.00037
- Filice, F., Blum, W., Lauber, E., and Schwaller, B. (2019). Inducible and reversible silencing of the Pvalb gene in mice: an *in vitro* and *in vivo* study. *Eur. J. Neurosci.* 50, 2694–2706. doi: 10.1111/ejn.14404
- Filice, F., Lauber, E., Vorckel, K. J., Wöhr, M., and Schwaller, B. (2018). 17-beta estradiol increases parvalbumin levels in Pvalb heterozygous mice and attenuates behavioral phenotypes with relevance to autism core symptoms. *Mol. Autism* 9:15. doi: 10.1186/s13229-018-0199-3
- Filice, F., Vorckel, K. J., Sungur, A. O., Wöhr, M., and Schwaller, B. (2016). Reduction in parvalbumin expression not loss of the parvalbumin-expressing GABA interneuron subpopulation in genetic parvalbumin and shank mouse models of autism. *Mol. Brain* 9:10. doi: 10.1186/s13041-016-0192-8
- Frankland, P. W., Wang, Y., Rosner, B., Shimizu, T., Balleine, B. W., Dykens, E. M., et al. (2004). Sensorimotor gating abnormalities in young males with fragile X syndrome and *Fmr1*-knockout mice. *Mol. Psychiatry* 9, 417–425. doi: 10.1038/sj.mp.4001432
- Frega, M., Selten, M., Mossink, B., Keller, J. M., Linda, K., Moerschen, R., et al. (2020). Distinct pathogenic genes causing intellectual disability and autism exhibit a common neuronal network hyperactivity phenotype. *Cell Rep.* 30, 173–186. doi: 10.1016/j.celrep.2019.12.002
- Fuccillo, M. V. (2016). Striatal circuits as a common node for autism pathophysiology. *Front. Neurosci.* 10:27. doi: 10.3389/fnins.2016.00027
- Fujimoto, N., Igarashi, K., Kanno, J., Honda, H., and Inoue, T. (2004). Identification of estrogen-responsive genes in the GH3 cell line by cDNA microarray analysis. *J. Steroid Biochem. Mol. Biol.* 91, 121–129. doi: 10.1016/j.jsbmb.2004.02.006
- Gala, R., Budzillo, A., Baftizadeh, F., Miller, J., Gouwens, N., Arkhipov, A., et al. (2020). Consistent cross-modal identification of cortical neurons with coupled autoencoders. *bioRxiv* doi: 10.1101/2020.06.30.181065
- Galarreta, M., and Hestrin, S. (1999). A network of fast-spiking cells in the neocortex connected by electrical synapses. *Nature* 402, 72–75. doi: 10.1038/47029
- Gandal, M. J., Edgar, J. C., Ehrlichman, R. S., Mehta, M., Roberts, T. P., and Siegel, S. J. (2010). Validating gamma oscillations and delayed auditory responses as translational biomarkers of autism. *Biol. Psychiatry* 68, 1100–1106. doi: 10.1016/j.biopsych.2010.09.031
- Gandal, M. J., Nesbitt, A. M., McCurdy, R. M., and Alter, M. D. (2012). Measuring the maturity of the fast-spiking interneuron transcriptional program in autism, schizophrenia, and bipolar disorder. *PLoS ONE* 7:e41215. doi: 10.1371/journal.pone.0041215
- Garbett, K., Ebert, P. J., Mitchell, A., Lintas, C., Manzi, B., Mirnics, K., et al. (2008). Immune transcriptome alterations in the temporal cortex of subjects with autism. *Neurobiol. Dis.* 30, 303–311. doi: 10.1016/j.nbd.2008.01.012
- Garrett, L., Chang, Y. J., Niedermeier, K. M., Heermann, T., Enard, W., Fuchs, H., et al. (2020). A truncating *Aspm* allele leads to a complex cognitive phenotype

- and region-specific reductions in parvalbuminergic neurons. *Transl. Psychiatry* 10:66. doi: 10.1038/s41398-020-0686-0
- Gibson, J. R., Bartley, A. F., Hays, S. A., and Huber, K. M. (2008). Imbalance of neocortical excitation and inhibition and altered UP states reflect network hyperexcitability in the mouse model of fragile X syndrome. *J. Neurophysiol.* 100, 2615–2626. doi: 10.1152/jn.90752.2008
- Gogolla, N., Leblanc, J. J., Quast, K. B., Sudhof, T. C., Fagiolini, M., and Hensch, T. K. (2009). Common circuit defect of excitatory-inhibitory balance in mouse models of autism. *J. Neurodev. Disord.* 1, 172–181. doi: 10.1007/s11689-009-9023-x
- Gogolla, N., Takesian, A. E., Feng, G., Fagiolini, M., and Hensch, T. K. (2014). Sensory integration in mouse insular cortex reflects GABA circuit maturation. *Neuron* 83, 894–905. doi: 10.1016/j.neuron.2014.06.033
- Gordon, A., Forsingdal, A., Klewe, I. V., Nielsen, J., Didriksen, M., Werge, T., et al. (2019). Transcriptomic networks implicate neuronal energetic abnormalities in three mouse models harboring autism and schizophrenia-associated mutations. *Mol. Psychiatry*. doi: 10.1038/s41380-019-0576-0
- Gouwens, N. W., Sorensen, S. A., Baftizadeh, F., Budzillo, A., Lee, B. R., Jarsky, T., et al. (2020). Toward an integrated classification of neuronal cell types: morphoelectric and transcriptomic characterization of individual GABAergic cortical neurons. *Cell*. 183:935–953.e19. doi: 10.1016/j.cell.2020.09.057
- Hardan, A. Y., Fung, L. K., Libove, R. A., Obukhanych, T. V., Nair, S., Herzenberg, L. A., et al. (2012). A randomized controlled pilot trial of oral N-acetylcysteine in children with autism. *Biol. Psychiatry* 71, 956–961. doi: 10.1016/j.biopsych.2012.01.014
- Hardingham, G. E., and Do, K. Q. (2016). Linking early-life NMDAR hypofunction and oxidative stress in schizophrenia pathogenesis. *Nat. Rev. Neurosci.* 17, 125–134. doi: 10.1038/nrn.2015.19
- Härtig, W., Brauer, K., and Bruckner, G. (1992). Wisteria floribunda agglutinin-labelled nets surround parvalbumin-containing neurons. *Neuroreport* 3, 869–872. doi: 10.1097/00001756-199210000-00012
- Hashemi, E., Ariza, J., Rogers, H., Noctor, S. C., and Martinez-Cerdeno, V. (2017). The number of parvalbumin-expressing interneurons is decreased in the prefrontal cortex in autism. *Cereb. Cortex* 27, 1931–1943. doi: 10.1093/cercor/bhw021
- Hashemi, E., Ariza, J., Rogers, H., Noctor, S. C., and Martinez-Cerdeno, V. (2018). The number of parvalbumin-expressing interneurons is decreased in the prefrontal cortex in autism. *Cereb. Cortex* 28:690. doi: 10.1093/cercor/bhx063
- Henzi, T., and Schwaller, B. (2015). Antagonistic regulation of parvalbumin expression and mitochondrial calcium handling capacity in renal epithelial cells. *PLoS ONE* 10:e0142005. doi: 10.1371/journal.pone.0142005
- Hodge, R. D., Bakken, T. E., Miller, J. A., Smith, K. A., Barkan, E. R., Graybuck, L. T., et al. (2019). Conserved cell types with divergent features in human versus mouse cortex. *Nature* 573, 61–68. doi: 10.1038/s41586-019-1506-7
- Hu, H., Gan, J., and Jonas, P. (2014). Interneurons. Fast-spiking, parvalbumin(+) GABAergic interneurons: from cellular design to microcircuit function. *Science* 345:1255263. doi: 10.1126/science.1255263
- Ito-Ishida, A., Ure, K., Chen, H., Swann, J. W., and Zoghbi, H. Y. (2015). Loss of MeCP2 in parvalbumin- and somatostatin-expressing neurons in mice leads to distinct rett syndrome-like phenotypes. *Neuron* 88, 651–658. doi: 10.1016/j.neuron.2015.10.029
- Janickova, L., Rechberger, K. F., Wey, L., and Schwaller, B. (2020). Absence of parvalbumin increases mitochondria volume and branching of dendrites in Pvalb neurons *in vivo*: a point of convergence of autism spectrum disorder (ASD) risk gene phenotypes. *Mol. Autism* 11:47. doi: 10.1186/s13229-020-00323-8
- Janickova, L., and Schwaller, B. (2020). Parvalbumin-deficiency accelerates the age-dependent ROS production in Pvalb neurons *in vivo*: link to neurodevelopmental disorders. *Front. Cell Neurosci.* 14:571216. doi: 10.3389/fncel.2020.571216
- Jaramillo, T. C., Xuan, Z., Reimers, J. M., Escamilla, C. O., Liu, S., and Powell, C. M. (2020). Early restoration of Shank3 expression in Shank3 knockout mice prevents core ASD-like behavioural phenotypes. *eNeuro*. doi: 10.1523/ENEURO.0332-19.2020
- Jurgensen, S., and Castillo, P. E. (2015). Selective dysregulation of hippocampal inhibition in the mouse lacking autism candidate gene CNTNAP2. *J. Neurosci.* 35, 14681–14687. doi: 10.1523/JNEUROSCI.1666-15.2015
- Kann, O. (2016). The interneuron energy hypothesis: implications for brain disease. *Neurobiol. Dis.* 90, 75–85. doi: 10.1016/j.nbd.2015.08.005
- Kann, O., Papageorgiou, I. E., and Draguhn, A. (2014). Highly energized inhibitory interneurons are a central element for information processing in cortical networks. *J. Cereb. Blood Flow Metab.* 34, 1270–1282. doi: 10.1038/jcbfm.2014.104
- Karayannis, T., Au, E., Patel, J. C., Markx, S., Delorme, R., et al. (2014). Cntnap4 differentially contributes to GABAergic and dopaminergic synaptic transmission. *Nature* 511, 236–240. doi: 10.1038/nature13248
- Kawaguchi, Y., and Kubota, Y. (1997). GABAergic cell subtypes and their synaptic connections in rat frontal cortex. *Cereb. Cortex* 7, 476–486. doi: 10.1093/cercor/7.6.476
- Kim, M. H., Korogod, N., Schneggenburger, R., Ho, W. K., and Lee, S. H. (2005). Interplay between Na⁺/Ca²⁺ exchangers and mitochondria in Ca²⁺ clearance at the calyx of Held. *J. Neurosci.* 25, 6057–6065. doi: 10.1523/JNEUROSCI.0454-05.2005
- Kim, Y., Yang, G. R., Pradhan, K., Venkataraju, K. U., Bota, M., Garcia Del Molino, L. C., et al. (2017). Brain-wide maps reveal stereotyped cell-type-based cortical architecture and subcortical sexual dimorphism. *Cell* 171, 456–469.e422. doi: 10.1016/j.cell.2017.09.020
- Kirischuk, S., and Grantyn, R. (2003). Intraterminal Ca²⁺ concentration and asynchronous transmitter release at single GABAergic boutons in rat collicular cultures. *J. Physiol.* 548, 753–764. doi: 10.1113/jphysiol.2002.037036
- Klauser, P., Xin, L., Fournier, M., Griffa, A., Cleusix, M., Jenni, R., et al. (2018). N-acetylcysteine add-on treatment leads to an improvement of fornix white matter integrity in early psychosis: a double-blind randomized placebo-controlled trial. *Transl. Psychiatry* 8:220. doi: 10.1038/s41398-018-0266-8
- Klug, J. R., Engelhardt, M. D., Cadman, C. N., Li, H., Smith, J. B., Ayala, S., et al. (2018). Differential inputs to striatal cholinergic and parvalbumin interneurons imply functional distinctions. *Elife* 7:e35657. doi: 10.7554/eLife.35657.020
- Krishnan, K., Wang, B. S., Lu, J., Wang, L., Maffei, A., Cang, J., et al. (2015). MeCP2 regulates the timing of critical period plasticity that shapes functional connectivity in primary visual cortex. *Proc. Natl. Acad. Sci. U. S. A.* 112, E4782–4791. doi: 10.1073/pnas.1506499112
- Krol, A., Wimmer, R. D., Halassa, M. M., and Feng, G. (2018). Thalamic reticular dysfunction as a circuit endophenotype in neurodevelopmental disorders. *Neuron* 98, 282–295. doi: 10.1016/j.neuron.2018.03.021
- Langen, M., Durston, S., Staal, W. G., Palmen, S. J., and Van Engeland, H. (2007). Caudate nucleus is enlarged in high-functioning medication-naïve subjects with autism. *Biol. Psychiatry* 62, 262–266. doi: 10.1016/j.biopsych.2006.09.040
- Lauber, E., Filice, F., and Schwaller, B. (2016). Prenatal valproate exposure differentially affects parvalbumin-expressing neurons and related circuits in the cortex and striatum of mice. *Front. Mol. Neurosci.* 9:150. doi: 10.3389/fnmol.2016.00150
- Lauber, E., Filice, F., and Schwaller, B. (2018). Dysregulation of parvalbumin expression in the cntnap2^{-/-} mouse model of autism spectrum disorder. *Front. Mol. Neurosci.* 11:262. doi: 10.3389/fnmol.2018.00262
- Leblanc, J. J., and Fagiolini, M. (2011). Autism: a “critical period” disorder? *Neural Plast.* 2011:921680. doi: 10.1155/2011/921680
- Lee, E., Lee, J., and Kim, E. (2017). Excitation/inhibition imbalance in animal models of autism spectrum disorders. *Biol. Psychiatry* 81, 838–847. doi: 10.1016/j.biopsych.2016.05.011
- Lee, S. H., Schwaller, B., and Neher, E. (2000). Kinetics of Ca²⁺ binding to parvalbumin in bovine chromaffin cells: implications for [Ca²⁺] transients of neuronal dendrites. *J. Physiol.* (525 Pt 2), 419–432. doi: 10.1111/j.1469-7793.2000.t01-2-00419.x
- Leonzino, M., Busnelli, M., Antonucci, F., Verderio, C., Mazzanti, M., and Chini, B. (2016). The timing of the excitatory-to-inhibitory GABA switch is regulated by the oxytocin receptor via KCC2. *Cell Rep.* 15, 96–103. doi: 10.1016/j.celrep.2016.03.013
- Li, W., and Pozzo-Miller, L. (2019). Dysfunction of the corticostriatal pathway in autism spectrum disorders. *J. Neurosci. Res.* 98:2130–2147. doi: 10.1002/jnr.24560
- Lichvarova, L., Blum, W., Schwaller, B., and Szabolcsi, V. (2019). Parvalbumin expression in oligodendrocyte-like CG4 cells causes a reduction in

- mitochondrial volume, attenuation in reactive oxygen species production and a decrease in cell processes' length and branching. *Sci. Rep.* 9:10603. doi: 10.1038/s41598-019-47112-9
- Lien, C. C., and Jonas, P. (2003). Kv3 potassium conductance is necessary and kinetically optimized for high-frequency action potential generation in hippocampal interneurons. *J. Neurosci.* 23, 2058–2068. doi: 10.1523/JNEUROSCI.23-06-02058.2003
- Lim, L., Mi, D., Llorca, A., and Marin, O. (2018). Development and functional diversification of cortical interneurons. *Neuron* 100, 294–313. doi: 10.1016/j.neuron.2018.10.009
- Lu, T., and Trussell, L. O. (2000). Inhibitory transmission mediated by asynchronous transmitter release. *Neuron* 26, 683–694. doi: 10.1016/S0896-6273(00)81204-0
- Maetzler, W., Nitsch, C., Bendfeldt, K., Racay, P., Vollenweider, F., and Schwaller, B. (2004). Ectopic parvalbumin expression in mouse forebrain neurons increases excitotoxic injury provoked by ibotenic acid injection into the striatum. *Exp. Neurol.* 186, 78–88. doi: 10.1016/j.expneurol.2003.10.014
- Manseau, F., Marinelli, S., Mendez, P., Schwaller, B., Prince, D. A., Huguenard, J. R., et al. (2010). Desynchronization of neocortical networks by asynchronous release of GABA at autaptic and synaptic contacts from fast-spiking interneurons. *PLoS Biol.* 8:e1000492. doi: 10.1371/journal.pbio.1000492
- Marin, O. (2012). Interneuron dysfunction in psychiatric disorders. *Nat. Rev. Neurosci.* 13, 107–120. doi: 10.1038/nrn3155
- Marino, M., Galluzzo, P., and Ascenzi, P. (2006). Estrogen signaling multiple pathways to impact gene transcription. *Curr. Genomics* 7, 497–508. doi: 10.2174/138920206779315737
- Markram, K., Rinaldi, T., La Mendola, D., Sandi, C., and Markram, H. (2008). Abnormal fear conditioning and amygdala processing in an animal model of autism. *Neuropsychopharmacology* 33, 901–912. doi: 10.1038/sj.npp.1301453
- Maurer, R. G., and Damasio, A. R. (1982). Childhood autism from the point of view of behavioral neurology. *J. Autism Dev. Disord.* 12, 195–205. doi: 10.1007/BF01531309
- McFarlane, H. G., Kusek, G. K., Yang, M., Phoenix, J. L., Bolivar, V. J., and Crawley, J. N. (2008). Autism-like behavioral phenotypes in BTBR T+tf/J mice. *Genes Brain Behav.* 7, 152–163. doi: 10.1111/j.1601-183X.2007.00330.x
- Mei, Y., Monteiro, P., Zhou, Y., Kim, J. A., Gao, X., Fu, Z., et al. (2016). Adult restoration of Shank3 expression rescues selective autistic-like phenotypes. *Nature* 530, 481–484. doi: 10.1038/nature16971
- Modi, B., Pimpinella, D., Paziienti, A., Zacchi, P., Cherubini, E., and Griguoli, M. (2019). Possible implication of the CA2 hippocampal circuit in social cognition deficits observed in the neuroligin 3 knock-out mouse, a non-syndromic animal model of autism. *Front. Psychiatry* 10:513. doi: 10.3389/fpsy.2019.00513
- Mootha, V. K., Bunkenborg, J., Olsen, J. V., Hjerrild, M., Wisniewski, J. R., Stahl, E., et al. (2003). Integrated analysis of protein composition, tissue diversity, and gene regulation in mouse mitochondria. *Cell* 115, 629–640. doi: 10.1016/S0092-8674(03)00926-7
- Morawski, M., Reinert, T., Meyer-Klaucke, W., Wagner, F. E., Troger, W., Reinert, A., et al. (2015). Ion exchanger in the brain: Quantitative analysis of perineuronally fixed anionic binding sites suggests diffusion barriers with ion sorting properties. *Sci. Rep.* 5:16471. doi: 10.1038/srep16471
- Muller, M., Felmy, F., Schwaller, B., and Schneggenburger, R. (2007). Parvalbumin is a mobile presynaptic Ca²⁺ buffer in the calyx of held that accelerates the decay of Ca²⁺ and short-term facilitation. *J. Neurosci.* 27, 2261–2271. doi: 10.1523/JNEUROSCI.5582-06.2007
- Negwer, M., Piera, K., Hesen, R., Lutje, L., Aarts, L., Schubert, D., et al. (2020). EHMT1 regulates Parvalbumin-positive interneuron development and GABAergic input in sensory cortical areas. *Brain Struct. Funct.* doi: 10.1007/s00429-020-02149-9
- Nelson, S. B., and Valakh, V. (2015). Excitatory/inhibitory balance and circuit homeostasis in autism spectrum disorders. *Neuron* 87, 684–698. doi: 10.1016/j.neuron.2015.07.033
- Nobili, A., Krashia, P., Cordella, A., La Barbera, L., Dell'acqua, M. C., Caruso, A., et al. (2018). Ambra1 shapes hippocampal inhibition/excitation balance: role in neurodevelopmental disorders. *Mol. Neurobiol.* 55, 7921–7940. doi: 10.1007/s12035-018-0911-5
- Oblak, A. L., Rosene, D. L., Kemper, T. L., Bauman, M. L., and Blatt, G. J. (2011). Altered posterior cingulate cortical cytoarchitecture, but normal density of neurons and interneurons in the posterior cingulate cortex and fusiform gyrus in autism. *Autism Res.* 4, 200–211. doi: 10.1002/aur.188
- Okaty, B. W., Miller, M. N., Sugino, K., Hempel, C. M., and Nelson, S. B. (2009). Transcriptional and electrophysiological maturation of neocortical fast-spiking GABAergic interneurons. *J. Neurosci.* 29, 7040–7052. doi: 10.1523/JNEUROSCI.0105-09.2009
- Orduz, D., Bishop, D. P., Schwaller, B., Schiffmann, S. N., and Gall, D. (2013). Parvalbumin tunes spike-timing and efferent short-term plasticity in striatal fast spiking interneurons. *J. Physiol.* 591, 3215–3232. doi: 10.1113/jphysiol.2012.250795
- Palmieri, L., and Persico, A. M. (2010). Mitochondrial dysfunction in autism spectrum disorders: cause or effect? *Biochim. Biophys. Acta* 1797, 1130–1137. doi: 10.1016/j.bbabi.2010.04.018
- Pangrazzi, L., Balasco, L., and Bozzi, Y. (2020). Oxidative stress and immune system dysfunction in autism spectrum disorders. *Int. J. Mol. Sci.* 21:3293. doi: 10.3390/ijms21093293
- Parikshak, N. N., Swarup, V., Belgard, T. G., Irimia, M., Ramaswami, G., Gandal, M. J., et al. (2016). Genome-wide changes in lncRNA, splicing, and regional gene expression patterns in autism. *Nature* 540, 423–427. doi: 10.1038/nature20612
- Patrizi, A., Awad, P. N., Chattopadhyaya, B., Li, C., Di Cristo, G., and Fagiolini, M. (2019). Accelerated hyper-maturation of parvalbumin circuits in the absence of MeCP2. *Cereb. Cortex.* 30, 256–268. doi: 10.1093/cercor/bhz085
- Peca, J., Feliciano, C., Ting, J. T., Wang, W., Wells, M. F., Venkatraman, T. N., et al. (2011). Shank3 mutant mice display autistic-like behaviours and striatal dysfunction. *Nature* 472, 437–442. doi: 10.1038/nature09965
- Penagarikano, O., Abrahams, B. S., Herman, E. I., Winden, K. D., Gdalyahu, A., Dong, H., et al. (2011). Absence of CNTNAP2 leads to epilepsy, neuronal migration abnormalities, and core autism-related deficits. *Cell* 147, 235–246. doi: 10.1016/j.cell.2011.08.040
- Pietro Paolo, S., Guillemot, A., Martin, B., D'amato, F. R., and Crusio, W. E. (2011). Genetic-background modulation of core and variable autistic-like symptoms in Fmr1 knock-out mice. *PLoS ONE* 6:e17073. doi: 10.1371/journal.pone.0017073
- Pirone, A., Viaggi, C., Cantile, C., Giannessi, E., Pardini, C., Vaglini, F., et al. (2020). Morphological alterations of the reticular thalamic nucleus in Engrailed-2 knockout mice. *J. Anat.* 236, 883–890. doi: 10.1111/joa.13150
- Polepalli, J. S., Wu, H., Goswami, D., Halpern, C. H., Sudhof, T. C., and Malenka, R. C. (2017). Modulation of excitation on parvalbumin interneurons by neuroligin-3 regulates the hippocampal network. *Nat. Neurosci.* 20, 219–229. doi: 10.1038/nn.4471
- Provenzano, G., Gilardoni, A., Maggia, M., Pernigo, M., Sgado, P., Casarosa, S., et al. (2020). Altered expression of GABAergic markers in the forebrain of young and adult Engrailed-2 knockout mice. *Genes* 11:384. doi: 10.3390/genes11040384
- Rapanelli, M., Frick, L. R., Xu, M. Y., Groman, S. M., Jindachomthong, K., Tamamaki, N., et al. (2017). Targeted interneuron depletion in the dorsal striatum produces autism-like behavioral abnormalities in male but not female mice. *Biol. Psychiatry* 82, 194–203. doi: 10.1016/j.biopsych.2017.01.020
- Reilly, M. P., Weeks, C. D., Topper, V. Y., Thompson, L. M., Crews, D., and Gore, A. C. (2015). The effects of prenatal PCBs on adult social behavior in rats. *Horm. Behav.* 73, 47–55. doi: 10.1016/j.yhbeh.2015.06.002
- Rettsa, C., Knebel, J. F., Geiser, E., Ferrari, C., Jenni, R., Fournier, M., et al. (2018). Treatment in early psychosis with N-acetyl-cysteine for 6 months improves low-level auditory processing: Pilot study. *Schizophr. Res.* 191, 80–86. doi: 10.1016/j.schres.2017.07.008
- Rothwell, P. E., Fuccillo, M. V., Maxeiner, S., Hayton, S. J., Gokce, O., Lim, B. K., et al. (2014). Autism-associated neuroligin-3 mutations commonly impair striatal circuits to boost repetitive behaviors. *Cell* 158, 198–212. doi: 10.1016/j.cell.2014.04.045
- Rubenstein, J. L., and Merzenich, M. M. (2003). Model of autism: increased ratio of excitation/inhibition in key neural systems. *Genes Brain Behav.* 2, 255–267. doi: 10.1034/j.1601-183X.2003.00037.x
- Satterstrom, F. K., Kosmicki, J. A., Wang, J. B., Breen, M. S., De Rubeis, S., An, J. Y., et al. (2020). Large-scale exome sequencing study implicates both developmental and functional changes in the neurobiology of autism. *Cell* 180:568. doi: 10.1016/j.cell.2019.12.036

- Scattoni, M. L., Ricceri, L., and Crawley, J. N. (2011). Unusual repertoire of vocalizations in adult BTBR T+tf/J mice during three types of social encounters. *Genes Brain Behav.* 10, 44–56. doi: 10.1111/j.1601-183X.2010.00623.x
- Schmidt, H., Stiefel, K. M., Racay, P., Schwaller, B., and Eilers, J. (2003). Mutational analysis of dendritic Ca²⁺ kinetics in rodent Purkinje cells: role of parvalbumin and calbindin D28k. *J. Physiol.* 551, 13–32. doi: 10.1113/jphysiol.2002.035824
- Schmitt, L. I., Wimmer, R. D., Nakajima, M., Happ, M., Mofakham, S., and Halassa, M. M. (2017). Thalamic amplification of cortical connectivity sustains attentional control. *Nature* 545, 219–223. doi: 10.1038/nature22073
- Schneider, T., and Przewlocki, R. (2005). Behavioral alterations in rats prenatally exposed to valproic acid: animal model of autism. *Neuropsychopharmacology* 30, 80–89. doi: 10.1038/sj.npp.1300518
- Schuetze, M., Cho, I. Y. K., Vinette, S., Rivard, K. B., Rohr, C. S., Ten Eycke, K., et al. (2019). Learning with individual-interest outcomes in Autism spectrum disorder. *Dev. Cogn. Neurosci.* 38:100668. doi: 10.1016/j.dcn.2019.100668
- Schuetze, M., Park, M. T., Cho, I. Y., Macmaster, F. P., Chakravarty, M. M., and Bray, S. L. (2016). Morphological alterations in the thalamus, striatum, and pallidum in autism spectrum disorder. *Neuropsychopharmacology* 41, 2627–2637. doi: 10.1038/npp.2016.64
- Schwaller, B. (2020). Cytosolic Ca²⁺ buffers are inherently Ca²⁺ signal modulators. *Cold Spring Harb. Perspect. Biol.* 12:a035543. doi: 10.1101/cshperspect.a035543
- Schwaller, B., Tetko, I. V., Tandon, P., Silveira, D. C., Vreugdenhil, M., Henzi, T., et al. (2004). Parvalbumin deficiency affects network properties resulting in increased susceptibility to epileptic seizures. *Mol. Cell. Neurosci.* 25, 650–663. doi: 10.1016/j.mcn.2003.12.006
- Schwede, M., Nagpal, S., Gandal, M. J., PARIKSHAK, N. N., Mirnics, K., Geschwind, D. H., et al. (2018). Strong correlation of downregulated genes related to synaptic transmission and mitochondria in post-mortem autism cerebral cortex. *J. Neurodev. Disord.* 10:18. doi: 10.1186/s11689-018-9237-x
- Selby, L., Zhang, C., and Sun, Q. Q. (2007). Major defects in neocortical GABAergic inhibitory circuits in mice lacking the fragile X mental retardation protein. *Neurosci. Lett.* 412, 227–232. doi: 10.1016/j.neulet.2006.11.062
- Selten, M., Van Bokhoven, H., and Nadif Kasri, N. (2018). Inhibitory control of the excitatory/inhibitory balance in psychiatric disorders. *Fl1000Res* 7:23. doi: 10.12688/fl1000research.12155.1
- Shipp, S. (2017). The functional logic of corticostriatal connections. *Brain Struct. Funct.* 222, 669–706. doi: 10.1007/s00429-016-1250-9
- Siddiqui, M. F., Elwell, C., and Johnson, M. H. (2016). Mitochondrial dysfunction in autism spectrum disorders. *Autism Open Access* 6:1000190. doi: 10.4172/2165-7890.1000190
- Soghomonian, J. J., Zhang, K., Reprakash, S., and Blatt, G. J. (2017). Decreased parvalbumin mRNA levels in cerebellar Purkinje cells in autism. *Autism Res.* 10, 1787–1796. doi: 10.1002/aur.1835
- Somogyi, P., and Klausberger, T. (2005). Defined types of cortical interneurone structure space and spike timing in the hippocampus. *J. Physiol.* 562, 9–26. doi: 10.1113/jphysiol.2004.078915
- Speed, H. E., Masiulis, I., Gibson, J. R., and Powell, C. M. (2015). Increased cortical inhibition in autism-linked neuroigin-3R451C mice is due in part to loss of endocannabinoid signaling. *PLoS ONE* 10:e0140638. doi: 10.1371/journal.pone.0140638
- Stephenson, D. T., O'Neill, S. M., Narayan, S., Tiwari, A., Arnold, E., Samaroo, H. D., et al. (2011). Histopathologic characterization of the BTBR mouse model of autistic-like behavior reveals selective changes in neurodevelopmental proteins and adult hippocampal neurogenesis. *Mol. Autism* 2:7. doi: 10.1186/2040-2392-2-7
- Stellet, P., Cabungcal, J. H., Bukhari, S. A., Ardelt, M. I., Pantazopoulos, H., Hamati, F., et al. (2017a). The thalamic reticular nucleus in schizophrenia and bipolar disorder: role of parvalbumin-expressing neuron networks and oxidative stress. *Mol. Psychiatry* 23, 2057–2065. doi: 10.1038/mp.2017.230
- Stellet, P., Cabungcal, J. H., Coyle, J., Didriksen, M., Gill, K., Grace, A. A., et al. (2017b). Oxidative stress-driven parvalbumin interneuron impairment as a common mechanism in models of schizophrenia. *Mol. Psychiatry* 22, 936–943. doi: 10.1038/mp.2017.47
- Stellet, P., Cabungcal, J. H., Monin, A., Dwir, D., O'donnell, P., Cuenod, M., et al. (2016). Redox dysregulation, neuroinflammation, and NMDA receptor hypofunction: a “central hub” in schizophrenia pathophysiology? *Schizophr. Res.* 176, 41–51. doi: 10.1016/j.schres.2014.06.021
- Stoner, R., Chow, M. L., Boyle, M. P., Sunkin, S. M., Mouton, P. R., Roy, S., et al. (2014). Patches of disorganization in the neocortex of children with autism. *N. Engl. J. Med.* 370, 1209–1219. doi: 10.1056/NEJMoa1307491
- Sztainberg, Y., Chen, H. M., Swann, J. W., Hao, S., Tang, B., Wu, Z., et al. (2015). Reversal of phenotypes in MECP2 duplication mice using genetic rescue or antisense oligonucleotides. *Nature* 528, 123–126. doi: 10.1038/nature16159
- Tabuchi, K., Blundell, J., Etherton, M. R., Hammer, R. E., Liu, X., Powell, C. M., et al. (2007). A neuroigin-3 mutation implicated in autism increases inhibitory synaptic transmission in mice. *Science* 318, 71–76. doi: 10.1126/science.1146221
- Takesian, A. E., Bogart, L. J., Lichtman, J. W., and Hensch, T. K. (2018). Inhibitory circuit gating of auditory critical-period plasticity. *Nat. Neurosci.* 21, 218–227. doi: 10.1038/s41593-017-0064-2
- Talley, E. M., Cribbs, L. L., Lee, J. H., Daud, A., Perez-Reyes, E., and Bayliss, D. A. (1999). Differential distribution of three members of a gene family encoding low voltage-activated (T-type) calcium channels. *J. Neurosci.* 19, 1895–1911. doi: 10.1523/JNEUROSCI.19-06-01895.1999
- Tang, G., Gutierrez Rios, P., Kuo, S. H., Akman, H. O., Rosoklija, G., Tanji, K., et al. (2013). Mitochondrial abnormalities in temporal lobe of autistic brain. *Neurobiol. Dis.* 54, 349–361. doi: 10.1016/j.nbd.2013.01.006
- Tepper, J. M., Tecuapetla, F., Koos, T., and Ibanez-Sandoval, O. (2010). Heterogeneity and diversity of striatal GABAergic interneurons. *Front. Neuroanat.* 4:150. doi: 10.3389/fnana.2010.00150
- Tewari, B. P., Chaunsali, L., Campbell, S. L., Patel, D. C., Goode, A. E., and Sontheimer, H. (2018). Perineuronal nets decrease membrane capacitance of peritumoral fast spiking interneurons in a model of epilepsy. *Nat. Commun.* 9:4724. doi: 10.1038/s41467-018-07113-0
- Toledo-Rodriguez, M., Blumenfeld, B., Wu, C., Luo, J., Attali, B., Goodman, P., et al. (2004). Correlation maps allow neuronal electrical properties to be predicted from single-cell gene expression profiles in rat neocortex. *Cereb. Cortex* 14, 1310–1327. doi: 10.1093/cercor/bbh092
- Toledo-Rodriguez, M., Goodman, P., Illic, M., Wu, C., and Markram, H. (2005). Neuropeptide and calcium-binding protein gene expression profiles predict neuronal anatomical type in the juvenile rat. *J. Physiol.* 567, 401–413. doi: 10.1113/jphysiol.2005.089250
- Tripathi, P. P., Sgado, P., Scali, M., Viaggi, C., Casarosa, S., Simon, H. H., et al. (2009). Increased susceptibility to kainic acid-induced seizures in Engrailed-2 knockout mice. *Neuroscience* 159, 842–849. doi: 10.1016/j.neuroscience.2009.01.007
- Van Den Bosch, L., Schwaller, B., Vleminckx, V., Meijers, B., Stork, S., Ruehlicke, T., et al. (2002). Protective effect of parvalbumin on excitotoxic motor neuron death. *Exp. Neurol.* 174, 150–161. doi: 10.1006/exnr.2001.7858
- Vogt, D., Cho, K. K. A., Shelton, S. M., Paul, A., Huang, Z. J., Sohal, V. S., et al. (2018). Mouse Cntnap2 and human CNTNAP2 ASD alleles cell autonomously regulate pv+ cortical interneurons. *Cereb. Cortex* 28, 3868–3879. doi: 10.1093/cercor/bhx248
- Voineagu, I., Wang, X., Johnston, P., Lowe, J. K., Tian, Y., Horvath, S., et al. (2011). Transcriptomic analysis of autistic brain reveals convergent molecular pathology. *Nature* 474, 380–384. doi: 10.1038/nature10110
- Vreugdenhil, M., Jefferys, J. G., Celio, M. R., and Schwaller, B. (2003). Parvalbumin-deficiency facilitates repetitive IPSCs and gamma oscillations in the hippocampus. *J. Neurophysiol.* 89, 1414–1422. doi: 10.1152/jn.00576.2002
- Wang, D., and Fawcett, J. (2012). The perineuronal net and the control of CNS plasticity. *Cell Tissue Res.* 349, 147–160. doi: 10.1007/s00441-012-1375-y
- Wang, Y., Dye, C. A., Sohal, V., Long, J. E., Estrada, R. C., Roztocil, T., et al. (2010). Dlx5 and Dlx6 regulate the development of parvalbumin-expressing cortical interneurons. *J. Neurosci.* 30, 5334–5345. doi: 10.1523/JNEUROSCI.5963-09.2010
- Wells, M. F., Wimmer, R. D., Schmitt, L. I., Feng, G., and Halassa, M. M. (2016). Thalamic reticular impairment underlies attention deficit in Ptchd1(Y/-) mice. *Nature* 532, 58–63. doi: 10.1038/nature17427
- Wen, T. H., Lovelace, J. W., Ethell, I. M., Binder, D. K., and Razak, K. A. (2019). Developmental changes in EEG phenotypes in a mouse model of fragile X syndrome. *Neuroscience* 398, 126–143. doi: 10.1016/j.neuroscience.2018.11.047
- Whitney, E. R., Kemper, T. L., Rosene, D. L., Bauman, M. L., and Blatt, G. J. (2009). Density of cerebellar basket and stellate cells in autism: evidence for a late developmental loss of Purkinje cells. *J. Neurosci. Res.* 87, 2245–2254. doi: 10.1002/jnr.22056

- Wink, L. K., Adams, R., Wang, Z. M., Klaunig, J. E., Plawewski, M. H., Posey, D. J., et al. (2016). A randomized placebo-controlled pilot study of N-acetylcysteine in youth with autism spectrum disorder. *Mol. Autism* 7:26. doi: 10.1186/s13229-016-0088-6
- Wöhr, M., Orduz, D., Gregory, P., Moreno, H., Khan, U., Vorckel, K. J., et al. (2015). Lack of parvalbumin in mice leads to behavioral deficits relevant to all human autism core symptoms and related neural morphofunctional abnormalities. *Transl. Psychiatry* 5:e525. doi: 10.1038/tp.2015.19
- Ye, Q., and Miao, Q. L. (2013). Experience-dependent development of perineuronal nets and chondroitin sulfate proteoglycan receptors in mouse visual cortex. *Matrix Biol.* 32, 352–363. doi: 10.1016/j.matbio.2013.04.001
- Yi, F., Danko, T., Botelho, S. C., Patzke, C., Pak, C., Wernig, M., et al. (2016). Autism-associated SHANK3 haploinsufficiency causes Ih channelopathy in human neurons. *Science* 352:aaf2669. doi: 10.1126/science.aaf2669
- Zhang, L., Qin, Z., Ricke, K. M., Cruz, S. A., Stewart, A. F. R., and Chen, H. H. (2020a). Hyperactivated PTP1B phosphatase in parvalbumin neurons alters anterior cingulate inhibitory circuits and induces autism-like behaviors. *Nat. Commun.* 11:1017. doi: 10.1038/s41467-020-14813-z
- Zhang, Y., Liu, C., Zhang, L., Zhou, W., Yu, S., Yi, R., et al. (2020b). Effects of propofol on electrical synaptic strength in coupling reticular thalamic GABAergic parvalbumin-expressing neurons. *Front. Neurosci.* 14:364. doi: 10.3389/fnins.2020.00364
- Zikopoulos, B., and Barbas, H. (2013). Altered neural connectivity in excitatory and inhibitory cortical circuits in autism. *Front. Hum. Neurosci.* 7:609. doi: 10.3389/fnhum.2013.00609

Conflict of Interest: The authors declare that the research was conducted in the absence of any commercial or financial relationships that could be construed as a potential conflict of interest.

Copyright © 2020 Filice, Janickova, Henzi, Bilella and Schwaller. This is an open-access article distributed under the terms of the Creative Commons Attribution License (CC BY). The use, distribution or reproduction in other forums is permitted, provided the original author(s) and the copyright owner(s) are credited and that the original publication in this journal is cited, in accordance with accepted academic practice. No use, distribution or reproduction is permitted which does not comply with these terms.